27. Miller SA, Dykes DD, Polesky HF. A simple salting out procedure for extracting DNA from human nucleated cells. Nucleic Acids Res 1988;16:1215.
28. Hakonarson H, Gulcher JR, Stefansson K. deCODE genetics, Inc. Pharmacogenomics 2003;4:209–215.
29. Taylor JD, Briley D, Nguyen Q, et al. Flow cytometric platform for high-throughput single nucleotide polymorphism analysis. Biotechniques 2001;30:661–669.
30. Abecasis GR, Cherny SS, Cookson WO, Cardon LR. Merlin–rapid analysis of dense genetic maps using sparse gene flow trees. Nat Genet 2002;30:97–101.
31. Cottingham RW Jr, Idury RM, Schaffer AA. Faster sequential genetic linkage computations. Am J Hum Genet 1993;53:252–263.
32. Nichols WC, Pankratz N, Hernandez D, et al. Genetic screening for a single common LRRK2 mutation in familial Parkinson's disease. Lancet 2005;365:410–412.
33. Deng H, Le W, Guo Y, Hunter CB, Xie W, Jankovic J. Genetic and clinical identification of Parkinson's disease patients with LRRK2 G2019S mutation. Ann Neurol 2005;57:933–934.
34. Fendri K, Kefi M, Hentati F, Amouri R. Genetic heterogeneity within a consanguineous family involving the LGMD 2D and the LGMD 2C genes. Neuromuscul Disord 2006;16:316–320.
35. Skipper L, Shen H, Chua E, et al. Analysis of LRRK2 functional domains in nondominant Parkinson disease. Neurology 2005;65:1319–1321.

to move her neck in all directions without limitations of range of motion. Blinking rate is normal and postural tremor of the hands has also disappeared.

## REFERENCES


1. Lim EC, Seet RC, Wilder-Smith EP, Ong BK. Dystonia gravidarum: a new entity? Mov Disord 2006;21:69–70.
2. Smith MS, Evatt ML. Movement disorders in pregnancy. Neurol Clin 2004;22:783–798.
3. Duane DD. Spasmodic torticollis: clinical and biologic features and their implications for focal dystonia. Adv Neurol 1988;50: 473–492.
4. Cersosimo MG, Bertoti A, Roca CU, Micheli F. Botulinum toxin in a case of hemimasticatory spasm with severe worsening during pregnancy. Clin Neuropharmacol 2004;27:6–8.
5. Nausieda PA, Koller WC, Weiner WJ, Klawans HL. Chorea induced by oral contraceptives. Neurology 1979;29:1605–1609.
6. Cogen PH, Zimmerman EA. Ovarian steroid hormones and cerebral function. Adv Neurol 1979;26:123–133.
7. Hruska RE, Silbergeld EK. Increased dopamine receptor sensitivity after estrogen treatment using the rat rotation model. Science 1980;208:1466–1468.
8. Miranda M, Cardoso F, Giovannoni G, Church A. Oral contraceptive induced chorea: another condition associated with anti–basal ganglia antibodies. J Neurol Neurosurg Psychiatry 2004;75:32–328.
9. Cardoso F. Chorea gravidarum. Arch Neurol 2002;59:868–870.
10. Deuschl G, Heinen F, Guschlbauer B, Schneider S, Glocker FX, Lucking CH. Hand tremor in patients with spasmodic torticollis. Mov Disord 1997;12:547–552.
11. Van Hartesveldt C, Joyce JN. Effects of estrogen on the basal ganglia. Neurosci Biobehav Rev 1986;10:1–14.
12. Epidemiologic Study of Dystonia in Europe (ESDE) Collaborative Group. Sex-related influences on the frequency and age of onset of primary dystonia. Neurology 1999;53:1871–1873.
13. Friedman A, Fahn S. Spontaneous remissions in spasmodic torticollis. Neurology 1986;36:398–400.


# Neuropsychiatric and Cognitive Features in Autosomal-Recessive Early Parkinsonism due to PINK1 Mutations


Lilach Ephraty, MD,[1] Omer Porat, MA,[2] David Israeli, MD,[3] Oren S. Cohen, MD,[1,2] Olga Tunkel, MD,[1,2] Shinar Yael, PhD,[1] Yasaku Hatano, MD,[4] Nobutaka Hattori, MD,[4] and Sharon Hassin-Baer, MD[1,2]*

[1]*Department of Neurology, The Sagol Neuroscience Center, Tel-Aviv University, Tel-Aviv, Israel*
[2]*Parkinson's Disease and Movement Disorders Clinic, The Sagol Neuroscience Center, Tel-Aviv University, Tel-Aviv, Israel*
[3]*Department of Psychiatry, Chaim Sheba Medical Center, Tel-Aviv University, Tel-Aviv, Israel*
[4]*Department of Neurology, Juntendo University School of Medicine, Tokyo, Japan*



***Abstract:*** **Autosomal-recessive early-onset Parkinsonism (AREP) due to *PINK1* mutations is characterized by an early-onset, slowly progressive disease, with a good response to levodopa. Psychiatric and cognitive disturbances associated with AREP have rarely been reported in the literature. We describe 2 brothers from a Jewish–Iraqi consanguineous family with a homozygous *PINK1* nonsense mutation. Both patients presented with anxiety and dysphoria accompanied by a gait disturbance that developed subsequently into a clinical depression. During the course of the disease, both developed drug-induced behavioral disturbances of the hedonistic homeostatic dysregulation type and 1 had drug-induced psychosis. The first patient had been diagnosed with mild mental retardation and during the 22 years of disease had further deteriorated; the second developed frontal-type dementia at an early age, 20 years after onset. Their father had a psychiatric disorder but no Parkinsonism. This report expands the phenotypic profile of *PINK1*-related disease, presenting unique psychiatric and cognitive features as part of the clinical picture.** © 2007 Movement Disorder Society



**Key words:** Parkinsonism; PINK1; hereditary; cognitive; neuropsychiatry


The important role of genetics in the etiology of Parkinson's disease (PD) is becoming increasingly recog-


*Correspondence to: Dr. Sharon Hassin-Baer, Department of Neurology and Parkinson's Disease and Movement Disorders Clinic, Sagol Neuroscience Center, Chaim Sheba Medical Center, Tel Hashomer, 52621, Israel. E-mail: shassin@post.tau.ac.il



Received 10 May 2006; Revised 28 September 2006; Accepted 3 October 2006

**Published online 26 January 2007 in Wiley InterScience (www.interscience.wiley.com). DOI: 10.1002/mds.21319**

nized.[1] At present, 10 loci have been identified, representing genomic regions linked to Mendelian forms of PD, five of which (PARK 1, 2, 6, 7, and 8) have been shown to contain gene mutations.[2–6] Among the autosomal-recessive early-onset parkinsonian (AREP) disorders, PTEN-induced kinase 1 or *PINK1* (PARK6) is the second in prevalence.[7] There have only been a handful of reports describing the clinical characteristics of patients with *PINK1*-associated disease.[1,8–12] The known clinical picture is one of an early-onset (18–56 years) parkinsonian syndrome, a universally excellent and sustained response to levodopa and a protracted course. Psychiatric symptoms, even late in the disease were reported infrequently.[8,9,12] Only 2 cases of patients with cognitive impairment were reported, and these conditions developed late in the course of their disease.[1,11] Here, we present 2 brothers from a Jewish–Iraqi consanguineous family with AREP caused by mutations in *PINK1*, with prominent early psychiatric and cognitive features.

## CASE 1

The younger brother, first presented at age 25 with anxiety and depressive symptoms, along with complaints of gait difficulties. The prominent psychiatric symptoms caused a 2-year delay in diagnosis of Parkinsonism. Finally, however, an asymmetrical parkinsonian syndrome without tremor was defined, accompanied by mild lower limb spasticity. Head computed tomography and work-up for Wilson's disease were normal. An excellent response to L-dopa and sleep benefit were reported early in the disease course. Motor fluctuations and mild dyskinesia began a year later. During the follow-up period, the patient remained single and unemployed, despite only minimal motor handicap in the first 15 years of disease. At present, 22 years after disease onset, the most significant motor features are gait disturbances with severe freezing of gait, mainly in the *off* state. His antiparkinsonian therapy includes 450 mg of L-dopa divided in seven doses, entacapone 600 mg, pergolide 0.75 mg, amantadine 200 mg, and trihexyphenidyl 3 mg. The patient is adherent with the medication (given borderline intelligence and impulsivity).

### Neurocognitive Profile

The patient had 9 years of formal education and had been diagnosed with mild mental retardation (IQ = 69) during his twenties. Because he never had a stable job or a long-term relationship, it is difficult to estimate the extent of cognitive deterioration. According to family members and the decline in his overall functioning, there has been a steady deterioration in his cognitive abilities. Present neuropsychological work-up shows major impairment in functions of the frontal network. The patient is impulsive with perseverations and marked mental slowness (see Table 1).

### Psychiatric Profile

Antisocial behavior and pathological gambling were documented several years before presentation. At onset of Parkinsonism, he suffered from depressed mood, fatigue, palpitations, and dizziness. At that time, the differential diagnosis included simple schizophrenia, affective disorder, and personality disorder. Several trials of antipsychotic drugs caused severe Parkinsonism, which led to hospitalization. These symptoms improved after withdrawal of the drugs. During the past 15 years, he has not been hospitalized. At present, he is treated with citalopram and clonazepam with a good effect.

## CASE 2

The elder brother, presented at age 33 with gait difficulties and anxiety (4 years after his brother). An asymmetrical parkinsonian syndrome without tremor was evident. Spasticity and sleep benefit were absent. There was an excellent response to L-dopa. Fluctuations and mild dyskinesia evolved after 3 years. After 18 years of disease, the most significant motor features are prominent motor fluctuations with major gait disturbances during *off* periods. His speech is severely dysarthric and he has mild dyskinesia. He is, at present, severely disabled due to dose failures during much of the day, and commonly uses a wheelchair while *off*. His daily treatment includes 750 mg of L-dopa divided in six doses, pergolide 0.75 mg, and amantadine 300 mg.

### Neurocognitive Profile

The patient had 9 years of formal education. He had been a carpenter and later a postman for several years. Five years ago, he was dismissed from his job as a clerk in the post office due to repeated mistakes and negligence. His wife also complained about his apathy and forgetfulness. Executive functions are impaired, and he exhibits mental slowness, perseverations, and impulsivity (see Table 1).

### Psychiatric Profile

The patient has a stable marriage and 3 healthy children. At the age of 33, he had an episode of mixed anxiety and depression along with complaints of "lower limb weakness" and was hospitalized in a psychiatric department. He suffered from a dysphoric mood, palpitations, and insomnia. He was treated with benzodiazepines with marked improvement. During the following years, he remained stable on antidepressant therapy. Four

**TABLE 1.** *Neuropsychological profile*

| Measure | Test name | Case 1* | Case 2 * |
|---|---|---|---|
| | MMSE | 28, ND > 25 | 27, ND > 25 |
| Language | Verbal fluency: | | |
| | Semantic (sum 3 cat.) | −2.2 | −3.1 |
| | Phonemic (sum 3 letters) | −0.73 | −1.9 |
| Attention | Digits WAIS (Forward+Backward) | −1 | −0.66 |
| | Digit symbol: | −2.33 | −2.33 |
| | Trail making A | −23.6, 0 errors | −27.2, 9 errors |
| | Trail making B | −7.4, 0 errors | −10, 14 errors |
| Verbal Memory | Rey AVLT: | | |
| | Trial I (immediate memory): | −1.15 | 0.66 |
| | Trial V (learning): | −2.84 | −2.2 |
| | List B: | −0.24 | −1.5 |
| | Interference: | −1.66 | −2.14 |
| | Delayed recall: | −1.83 | −2.2 |
| | Delayed recognition: | −4.1 | – |
| Visuo-spatial | Rey Complex Figure | | |
| | Copying | −1.33 | −1 |
| | Immediate recall | −1.33 | −0.33 |
| | Delayed recall | −1.67 | −0.33 |
| | Block design: | −1.33 | −2 |
| | Hooper VOT | −8.2 | −5.9 |
| Executive Functions | Comprehension (WAIS III) | 0 | −0.67 |
| | Frontal Assessment Battery | 15, ND > 15 | 7, ND > 15 |
| | Stroop test, interference | −1.6 | −0.8 |
| | WCST | | |
| | Correct responses: | −22.67 | −21.67 |
| | Perseverative errors: | −21 | −23 |
| | Nonperseverative errors: | −11 | −21.3 |
| | Categories: | 2, ND = 6 | 3, ND = 6 |

Data are presented as Z scores. Case 1: 52 years old, 9 years of education. Case 2: 47 years old, 9 years of education.
ND, normative data; MMSE, Mini-Mental State Examination; WAIS, Wechsler Adult Intelligence Scale; AVLT, Auditory Verbal Learning Test; VOT, Visual Organization Test; WCST, Wisconsin Card Sorting Test.

years ago, severe drug-induced behavioral disturbances appeared, characterized by hypomanic behavior and hypersexuality. His behavior was typical of the hedonistic homeostatic dysregulation (HHD)[13] with punding behavior. His behavior further worsened, and he became disinhibited and aggressive, with thoughts of grandeur. He did not respond to reduction of dopamine agonist dosage or quetiapine and was hospitalized. His symptoms improved after treatment with clozapine. Psychiatric treatment today consists of clozapine 50 mg, fluoxetine 20 mg, and clonazepam 3 mg.

### Family History

The family history is negative for Parkinsonism. The patient's father suffered from an unspecific psychiatric disorder, most probably a schizoaffective disorder. Case 2 has a healthy twin sister. No other information is available (Fig. 1).

### Molecular Analysis

Linkage analysis was negative for *Parkin* and *DJ-1* mutations. Both patients are homozygous for a nonsense

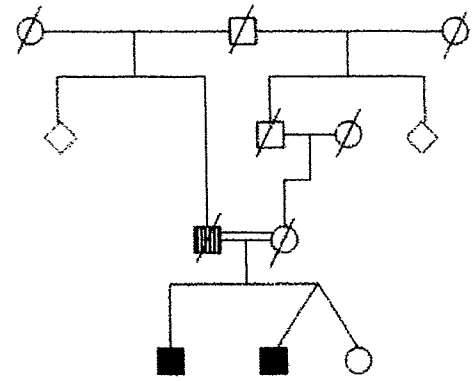

**FIG. 1.** Square symbols represent men, circles represent women, diamonds represent unknown number and gender of siblings, and diagonal lines indicate deceased individuals. The pedigree shows that 2 of the 3 siblings are affected (black squares). Both showed a homozygous nonsense mutation in exon 3 (nucleotide 736 C-to-T transition) in *PINK1*. The vertically hatched square shows the father who had a psychiatric disorder (information from history only).

mutation in exon 3 (nucleotide 736 C-to-T transition) in *PINK1*. This mutation was not present in DNA from 50 control Israeli patients of Jewish–Iraqi descent. It probably leads to premature termination and formation of a truncated protein that lacks 336 amino acids, including a highly conserved protein kinase domain. Genetic analysis is described elsewhere.[8]

## DISCUSSION

We present two brothers from a consanguineous family with AREP due to a homozygous mutation in *PINK1*. Both patients presented with psychiatric complaints accompanied by a gait disturbance. The psychiatric features were the major cause of disability in both patients. Both presented with anxiety and dysphoria developing subsequently into depression. Psychiatric disturbances were apparent before introduction of antiparkinsonian therapy. Although the first patient was diagnosed with mild mental retardation, during 22 years of disease he deteriorated and like his brother, developed dementia at an early age. Case 2 had no history of mental retardation. He developed an extensive cognitive decline involving damage to the frontal lobe network. Although a formal neuropsychological profile was completed only recently (Table 1), a long-standing cognitive deterioration was apparent over the years as the brothers' level of functioning declined and they became increasingly dependent. This finding was largely due to cognitive and psychiatric, rather than motor, disturbances.

Few studies describe the clinical features of AREP patients with *PINK1* mutations, and the phenotype is still being elucidated. Bonifati and colleagues recently described the clinical and genetic characteristics of 10 patients of which 5 had concomitant anxiety and/or depression.[9] Two additional patients in his series developed drug-induced hallucinations. Hatano and associates reported 2 other patients with hallucinations, although it was not mentioned whether these were drug induced.[8] Ibanez and coworkers described 12 patients, 3 of whom suffered from depression. In 1 patient, depression was diagnosed 20 years after parkinsonian symptoms. In the other 2, depression preceded parkinsonian symptoms by several years; of interest, these patients were sisters, both had the same homozygous mutation (Q456X).[12]

Two patients with cognitive impairment were reported. Healy and colleagues[11] described a woman of 64 years of age that developed dementia and visual hallucinations 13 years after disease onset. Li and associates[14] described a patient with dementia, depression, and hallucinations. Apart from these reports, dementia has not yet been described in patients with *PINK1* mutations.

The father of our patients suffered from an unspecified psychiatric disorder without parkinsonian features, suggesting that the *PINK1* mutation hemizygous state may be associated with psychiatric disturbances. Alternatively, a different genetic trait may contribute to the psychiatric disturbances in our patients and their father. To further explore the possibility of psychiatric disorders attributed to the hemizygous mutation state, family members of PD patients due to *PINK1* mutations should be screened for psychiatric symptoms.

This report expands the phenotypic profile of *PINK1*-related Parkinsonism, presenting unique psychiatric and cognitive features as part of the core clinical features of this disease. Variability in the phenotype of *PINK1* mutations highlights the overlap of clinical features in the three known recessive forms of young-onset Parkinsonism, stressing the need for genetic testing for accurate diagnosis.

## REFERENCES


1. Albanese A, Valente EM, Romito LM, et al. The PINK1 phenotype can be indistinguishable from idiopathic Parkinson disease. Neurology 2005;64:1958–1960.
2. Lewthwaite AJ, Nicholl DJ. Genetics of parkinsonism. Curr Neurol Neurosci Rep 2005;5:397–404.
3. Bonifati V. Genetics of Parkinson's disease. Minerva Med 2005; 96:175–186.
4. McInerney-Leo A, Hadley DW, Gwinn-Hardy K, et al. Genetic testing in Parkinson's disease. Mov Disord 2005;20:1–10.
5. Lucking CB, Durr A, Bonifati V, et al. Association between early-onset Parkinson's disease and mutations in the parkin gene. French Parkinson's Disease Genetics Study Group. N Engl J Med 2000;342:1560–1567.
6. Bonifati V, Rizzu P, van Baren MJ, et al. Mutations in the DJ-1 gene associated with autosomal recessive early-onset parkinsonism. Science 2003;299:256–259.
7. Valente EM, Abou-Sleiman PM, Caputo V, et al. Hereditary early-onset Parkinson's disease caused by mutations in PINK1. Science 2004;304:1158–1160.
8. Hatano Y, Sato K, Elibol B, et al. PARK6-linked autosomal recessive early-onset parkinsonism in Asian populations. Neurology 2004;63:1482–1485.
9. Bonifati V, Rohe CF, Breedveld GJ, et al. Early-onset parkinsonism associated with PINK1 mutations: frequency, genotypes, and phenotypes. Neurology 2005;65:87–95.
10. Valente EM, Salvi S, Ialongo T, et al. PINK1 mutations are associated with sporadic early-onset parkinsonism. Ann Neurol 2004;56:336–341.
11. Healy DG, Abou-Sleiman PM, Gibson JM, et al. PINK1 (PARK6) associated Parkinson disease in Ireland. Neurology 2004;63:1486–1488.
12. Ibanez P, Lesage S, Lohmann E, et al. Mutational analysis of the PINK1 gene in early-onset parkinsonism in Europe and North Africa. Brain 2006;129:686–694.
13. Pezzella FR, Colosimo C, Vanacore N, et al. Prevalence and clinical features of hedonistic homeostatic dysregulation in Parkinson's disease. Mov Disord 2005;20:77–81.
14. Li Y, Tomiyama H, Sato K, et al. Clinicogenetic study of *PINK1* mutations in autosomal recessive early-onset Parkinsonism. Neurology 2005;64:1955–1957.

# *Leucine-Rich Repeat kinase* 2 G2385R variant is a risk factor for Parkinson disease in Asian population

Manabu Funayama[a], Yuanzhe Li[b], Hiroyuki Tomiyama[b], Hiroyo Yoshino[a], Yoko Imamichi[b], Mitsutoshi Yamamoto[c,f], Miho Murata[d,f], Tatsushi Toda[e,f], Yoshikuni Mizuno[a] and Nobutaka Hattori[a,b,f]

[a]Research Institute for Diseases of Old Age, [b]Department of Neurology, Juntendo University School of Medicine, Bunkyo-ku, Tokyo, [c]Department of Neurology, Kagawa Prefectural Central Hospital, Takamatsu, [d]Department of Neurology, Musashi Hospital, National Center of Neurology and Psychiatry, Tokyo, [e]Division of Clinical Genetics, Department of Medical Genetics, Osaka University Graduate School of Medicine, Suita, Osaka and [f]Core Research for Evolutional Science and Technology (CREST), Japan Science and Technology Agency, Saitama, Japan

Correspondence and requests for reprints to Dr/Professor Nobutaka Hattori, MD, PhD, Department of Neurology, Juntendo University School of Medicine, 2-1-1 Hongo, Bunkyo-ku, Tokyo 113-8421, Japan
Tel: +81 3 5802 1073; fax: +81 3 5800 0547; e-mail: nhattori@med.juntendo.ac.jp

Sponsorship: This study was supported by a grant from the Japan Foundation for Neuroscience and Mental Health (to M.F.).

Received 10 October 2006; accepted 23 October 2006

To assess the effect of genetic factors on sporadic Parkinson disease, we performed a case–control study of a variant (G2385R) in *Leucine-Rich Repeat kinase* 2 among the Japanese population. The G2385R (c.7153G > A) variant was reported as a risk factor for sporadic Parkinson disease in the Chinese population from Taiwan and Singapore. Genotyping was conducted in 448 Parkinson disease patients and 457 healthy controls. The frequency of A allele in Parkinson disease was significantly higher than in the control ($P=1.24 \times 10^{-4}$, odds ratio 2.63, 95% confidence interval 1.56–4.35). Our results suggest that the G2385R variant is a risk factor for sporadic Parkinson disease in the Asian population. *NeuroReport* 18:273–275 © 2007 Lippincott Williams & Wilkins.

**Keywords:** *Leucine-Rich Repeat kinase 2*, risk factor, single nucleotide polymorphisms

## Introduction

Parkinson disease (PD) is one of the most frequent neurodegenerative diseases characterized by resting tremor, rigidity, bradykinesia, and postural instability. PD is thought to be a multifactorial disease caused by a combination of aging, environmental, and genetic factors. Although the majority of patients of PD are of sporadic type, some genes have been identified as a monogenic causative gene by molecular genetic studies for familial PD [1–6]. *Leucine-Rich Repeat kinase* 2 (*LRRK2*) has been identified as a causative gene associated with autosomal dominant familial PD [7,8]. To date, many pathogenic substitutions in *LRRK2* have been identified in familial and sporadic PD [9]. The G2385R variant (c.7153G>A) in *LRRK2* was reported recently as a risk factor for sporadic PD in the Chinese population from Taiwan and Singapore [10,11]. This variant was identified originally as putative pathogenic mutation in a small Taiwanese PD family and was not found in Caucasians [12]. Thus, it is possible that the G2385R variant is a risk factor in Asian sporadic PD. To test this hypothesis, we conducted a case–control study to evaluate the association between the G2385R genotype and the risk for PD in the Japanese population.

## Methods

### Subjects and genomic DNA

Genomic DNA was isolated from 448 sporadic PD patients and 457 controls of the Japanese population by a standard protocol (Table 1). All PD patients had no family history of PD. PD patients with *parkin* or *PTEN-induced putative kinase 1 (PINK1)* mutation were not included in the study. Diagnosis of PD was adopted by the participating neurologists and was established on the basis of the United Kingdom Parkinson's Disease Society Brain Bank criteria [13]. This study was approved by the ethics committee of Juntendo University School of Medicine. All individuals gave an informed and signed consent form.

### Genotyping

Exon 48 of *LRRK2* from each individual was amplified by polymerase chain reaction (PCR) using the primers and protocol described by Zimprich *et al.* [8]. The PCR products were sequenced directly using the BigDye Terminators v1.1 Cycle Sequencing Kit (Applied Biosystems, Foster City, California, USA). The reverse PCR primer was used as sequencing primer.

### Statistical analysis

Statistical analysis included the Hardy–Weinberg equilibrium test, $\chi^2$ test, Fisher's exact test, odds ratio and its 95% confidence interval (95% CI), using SNPAlyze v5.1 software (Dynacom, Chiba, Japan). The *t*-test was performed using JMP 6.0 (SAS Institute Japan, Tokyo, Japan). In all statistical analyses, *P* values of 0.05 or less were considered statistically significant.

## Results

We analyzed the frequency of the c.7153G>A (G2385R) substitution in 448 patients and 457 controls. Genotypes of the controls and patients were concordant with Hardy–Weinberg equilibrium. The frequency of A allele in the patients was significantly higher than in the controls ($P=1.24\times10^{-4}$, odds ratio 2.63, 95% CI 1.56–4.35, Table 2). We also detected homozygous substitution for the G2385R variant in two patients; however, we detected only the heterozygous substitution in the controls. Concerning the age at onset, the G2385R carriers were somewhat older than the noncarriers in total patients and in those <50 years of age. In contrast, the age at onset was not significantly different between carriers and noncarriers aged ≥50 years (Table 3). The disease duration was not significantly different between carriers and noncarriers (data not shown).

## Discussion

In this study, we observed the *LRRK2* G2385R variant in 11.6% (52/448) of sporadic PD patients. So far, many putative pathogenic mutations have been reported including the G2385R. We detected G2385R in both patients and controls (22/457: 4.8%, Table 2); thus, this variant is not a pathogenic mutation, but a single nucleotide polymorphism. These results were similar to the allele frequencies in the Chinese [10,11]. It is estimated that mutations of *LRRK2* are the most frequent among the causative genes for autosomal dominant familial PD so far. Indeed, only one mutation (G2019S) accounted for ~6.6% of familial PD and ~1.6% of sporadic PD in Caucasians [14–16]. Interestingly, the frequency of the G2019S mutation is ~40% in the familial PD of North African Arabs [17] and ~30% in the familial PD of Ashkenazi Jews [18], whereas the G2019S mutation is a much less common mutation in Asians [19,20]. It is likely that some differences of genetic background exist among Caucasians, North African Arabs, Ashkenazi Jews, and Asians. Although G2385R has been detected only in Asian population, some risk variations in PD such as α-synuclein would be found in not only Asians but also all ethnic groups [21–24].

Among patients with age at onset <50 years, the G2385R carriers were somewhat older than noncarriers. This might indicate that G2385R has no influence on early-onset PD, and that PD of patients with early-onset might be influenced by other genetic and/or environmental factors. In addition, there were no differences in any clinical features including age at onset among carriers with homozygous or heterozygous G2385R substitution and noncarriers. Although the G2385R might increase the risk of development of PD, it does not seem to have a clear effect on modifying the symptoms or worsening the progression of the disease.

The amino-acid G2385 is located in the WD domain of LRRK2. This domain is known to bind various proteins [9]. The WD domain of LRRK2 appears to play an important role in neuronal cells. Indeed, oxidative-stress-induced cell death was more enhanced by the overexpression of G2385R variant than wild-type LRRK2 using culture cells [11]. More studies are needed to understand the functional significance of the substitution of glycine to arginine.

## Conclusion

In this study, we identified that the G2385R variant in *LRRK2* is a risk for PD in Japanese population. To combine with the result of Chinese population [10,11], this variant increases the risk of PD in Asian population. So far, multiple genomic loci have been identified as susceptibility loci for PD [25], suggesting that many genes have a synergistic influence on the development of PD.

**Table 1** Age characteristics of individuals

| | Patients | Controls |
|---|---|---|
| Total sample, *n* (%) | 448 (100) | 457 (100) |
| Male, *n* (%) | 217 (48.4) | 240 (52.5) |
| Female, *n* (%) | 231 (51.6) | 217 (47.5) |
| Age at onset (years)[a] | 50.7 ± 14.6 (5–89) | — |
| Male[a] | 49.1 ± 14.8 (5–89) | — |
| Female[a] | 52.2 ± 14.2 (7–82) | — |
| Age at sampling (years)[a] | 59.4 ± 13.8 (15–93) | 43.8 ± 16.0 (21–98) |
| Male[a] | 57.8 ± 14.7 (15–93) | 43.8 ± 14.5 (23–92) |
| Female[a] | 60.9 ± 12.7 (22–88) | 43.9 ± 17.5 (21–98) |

[a]Data are mean ± SD (range).

**Table 3** Comparison of age at onset of PD patients

| Age at onset (years) | Carriers (*n*) | Noncarriers (*n*) | *P*-value |
|---|---|---|---|
| <50 | 42.5 ± 5.8 (17) | 37.1 ± 9.4 (180) | 0.003 |
| ≥50 | 59.9 ± 7.0 (33) | 61.6 ± 7.8 (209) | 0.24 |
| Total | 54.0 ± 10.6 (50) | 50.3 ± 14.9 (389) | 0.03 |

Data are mean ± SD.
Patients without information about age at onset (two of carriers and seven of noncarriers) were excluded from this analysis.
PD, Parkinson disease.

**Table 2** Association analysis of *LRRK2* G2385R variant

| | Genotype, *n* (%) | | | Allele, *n* (%) | | | |
|---|---|---|---|---|---|---|---|
| | G/G | G/A | A/A | G | A | $\chi^{2}$ [a] | *P*-value[a] |
| Patients (*n*=448) | 396 (88.4) | 50 (11.2) | 2 (0.4) | 842 (94.0) | 54 (6.0) | 14.74 | $1.24\times10^{-4}$ |
| Controls (*n*=457) | 435 (95.2) | 22 (4.8) | 0 (0) | 892 (97.6) | 22 (2.4) | | |

*LRRK2*, Leucine-Rich Repeat kinase 2.
[a]Compared with the control.

## References


1. Polymeropoulos MH, Lavedan C, Leroy E, Ide SE, Dehejia A, Dutra A, *et al.* Mutation in the alpha-synuclein gene identified in families with Parkinson's disease. *Science* 1997; **276**:2045–2047.
2. Kitada T, Asakawa S, Hattori N, Matsumine H, Yamamura Y, Minoshima S, *et al.* Mutations in the parkin gene cause autosomal recessive juvenile parkinsonism. *Nature* 1998; **392**:605–608.
3. Leroy E, Boyer R, Auburger G, Leube B, Ulm G, Mezey E, *et al.* The ubiquitin pathway in Parkinson's disease. *Nature* 1998; **395**:451–452.
4. Bonifati V, Rizzu P, van Baren MJ, Schaap O, Breedveld GJ, Krieger E, *et al.* Mutations in the DJ-1 gene associated with autosomal recessive early-onset parkinsonism. *Science* 2003; **299**:256–259.
5. Singleton AB, Farrer M, Johnson J, Singleton A, Hague S, Kachergus J, *et al.* Alpha-synuclein locus triplication causes Parkinson's disease. *Science* 2003; **302**:841.
6. Valente EM, Abou-Sleiman PM, Caputo V, Muqit MM, Harvey K, Gispert S, *et al.* Hereditary early-onset Parkinson's disease caused by mutations in PINK1. *Science* 2004; **304**:1158–1160.
7. Paisan-Ruiz C, Jain S, Evans EW, Gilks WP, Simon J, van der Brug M, *et al.* Cloning of the gene containing mutations that cause PARK8-linked Parkinson's disease. *Neuron* 2004; **44**:595–600.
8. Zimprich A, Biskup S, Leitner P, Lichtner P, Farrer M, Lincoln S, *et al.* Mutations in LRRK2 cause autosomal-dominant parkinsonism with pleomorphic pathology. *Neuron* 2004; **44**:601–607.
9. Mata IF, Wedemeyer WJ, Farrer MJ, Taylor JP, Gallo KA. LRRK2 in Parkinson's disease: protein domains and functional insights. *Trends Neurosci* 2006; **29**:286–293.
10. Di Fonzo A, Wu-Chou YH, Lu CS, van Doeselaar M, Simons EJ, Rohe CF, *et al.* A common missense variant in the LRRK2 gene, Gly2385Arg, associated with Parkinson's disease risk in Taiwan. *Neurogenetics* 2006; **7**:133–138.
11. Tan EK, Zhao Y, Skipper L, Tan MG, Di Fonzo A, Sun L, *et al.* The LRRK2 Gly2385Arg variant is associated with Parkinson's disease: genetic and functional evidence. *Hum Genet* 2006; Sep 30 [Epub ahead of print].
12. Mata IF, Kachergus JM, Taylor JP, Lincoln S, Aasly J, Lynch T, *et al.* Lrrk2 pathogenic substitutions in Parkinson's disease. *Neurogenetics* 2005; **6**:171–177.
13. Hughes AJ, Daniel SE, Kilford L, Lees AJ. Accuracy of clinical diagnosis of idiopathic Parkinson's disease: a clinico-pathological study of 100 cases. *J Neurol Neurosurg Psychiatry* 1992; **55**:181–184.
14. Nichols WC, Pankratz N, Hernandez D, Paisan-Ruiz C, Jain S, Halter CA, *et al.* Genetic screening for a single common LRRK2 mutation in familial Parkinson's disease. *Lancet* 2005; **365**:410–412.
15. Gilks WP, Abou-Sleiman PM, Gandhi S, Jain S, Singleton A, Lees AJ, *et al.* A common LRRK2 mutation in idiopathic Parkinson's disease. *Lancet* 2005; **365**:415–416.
16. Di Fonzo A, Rohe CF, Ferreira J, Chien HF, Vacca L, Stocchi F, *et al.* A frequent LRRK2 gene mutation associated with autosomal dominant Parkinson's disease. *Lancet* 2005; **365**:412–415.
17. Lesage S, Durr A, Tazir M, Lohmann E, Leutenegger AL, Janin S, *et al.* LRRK2 G2019S as a cause of Parkinson's disease in North African Arabs. *N Engl J Med* 2006; **354**:422–423.
18. Ozelius LJ, Senthil G, Saunders-Pullman R, Ohmann E, Deligtisch A, Tagliati M, *et al.* LRRK2 G2019S as a cause of Parkinson's disease in Ashkenazi Jews. *N Engl J Med* 2006; **354**:424–425.
19. Tan EK, Shen H, Tan LC, Farrer M, Yew K, Chua E, *et al.* The G2019S LRRK2 mutation is uncommon in an Asian cohort of Parkinson's disease patients. *Neurosci Lett* 2005; **384**:327–329.
20. Tomiyama H, Li Y, Funayama M, Hasegawa K, Yoshino H, Kubo SI, *et al.* Clinicogenetic study of mutations in LRRK2 exon 41 in Parkinson's disease patients from 18 countries. *Mov Disord* 2006; **21**: 1102–1108.
21. Farrer M, Maraganore DM, Lockhart P, Singleton A, Lesnick TG, de Andrade M, *et al.* Alpha-synuclein gene haplotypes are associated with Parkinson's disease. *Hum Mol Genet* 2001; **10**: 1847–1851.
22. Pals P, Lincoln S, Manning J, Heckman M, Skipper L, Hulihan M, *et al.* Alpha-synuclein promoter confers susceptibility to Parkinson's disease. *Ann Neurol* 2004; **56**:591–595.
23. Mueller JC, Fuchs J, Hofer A, Zimprich A, Lichtner P, Illig T, *et al.* Multiple regions of alpha-synuclein are associated with Parkinson's disease. *Ann Neurol* 2005; **57**:535–541.
24. Mizuta I, Satake W, Nakabayashi Y, Ito C, Suzuki S, Momose Y, *et al.* Multiple candidate gene analysis identifies alpha-synuclein as a susceptibility gene for sporadic Parkinson's disease. *Hum Mol Genet* 2006; **15**:1151–1158.
25. Maraganore DM, de Andrade M, Lesnick TG, Strain KJ, Farrer MJ, Rocca WA, *et al.* High-resolution whole-genome association study of Parkinson disease. *Am J Hum Genet* 2005; **77**:685–693.

Neuron
Article

# Sept4, a Component of Presynaptic Scaffold and Lewy Bodies, Is Required for the Suppression of α-Synuclein Neurotoxicity

Masafumi Ihara,[1,*] Nobuyuki Yamasaki,[2] Akari Hagiwara,[1] Ai Tanigaki,[6] Ayumi Kitano,[1] Rie Hikawa,[1] Hidekazu Tomimoto,[3] Makoto Noda,[4] Masashi Takanashi,[5] Hideo Mori,[5] Nobutaka Hattori,[5] Tsuyoshi Miyakawa,[2] and Makoto Kinoshita[1,6,*]
[1] Biochemistry and Cell Biology Unit, HMRO, Kyoto University Graduate School of Medicine, Yoshida Konoe, Sakyo, Kyoto 606-8501, Japan
[2] Genetic Engineering and Functional Genomics Unit, HMRO, Kyoto University Graduate School of Medicine, Yoshida Konoe, Sakyo, Kyoto 606-8501, Japan
[3] Department of Neurology, Kyoto University Graduate School of Medicine, Yoshida Konoe, Sakyo, Kyoto 606-8501, Japan
[4] Department of Molecular Oncology, Kyoto University Graduate School of Medicine, Yoshida Konoe, Sakyo, Kyoto 606-8501, Japan
[5] Department of Neurology, Juntendo University School of Medicine, Hongo, Bunkyo, Tokyo 113-8431, Japan
[6] PRESTO, Japan Science and Technology Agency, Honcho, Kawaguchi, Saitama 332-0012, Japan
*Correspondence: ihara@kuhp.kyoto-u.ac.jp (M.I.), mkinoshita@hmro.med.kyoto-u.ac.jp (M.K.)
DOI 10.1016/j.neuron.2007.01.019

## SUMMARY

**In Parkinson disease (PD), α-synuclein aggregates called Lewy bodies often involve and sequester Septin4 (Sept4), a polymerizing scaffold protein. However, the pathophysiological significance of this phenomenon is unclear. Here, we show the physiological association of Sept4 with α-synuclein, the dopamine transporter, and other presynaptic proteins in dopaminergic neurons; mice lacking Sept4 exhibit diminished dopaminergic neurotransmission due to scarcity of these presynaptic proteins. These data demonstrate an important role for septin scaffolds in the brain. In transgenic mice that express human α-synuclein$^{A53T}$ (a mutant protein responsible for familial PD), loss of Sept4 significantly enhances neuropathology and locomotor deterioration. In this PD model, insoluble deposits of Ser$^{129}$-phosphorylated α-synuclein$^{A53T}$ are negatively correlated with the dosage of Sept4. In vitro, direct association with Sept4 protects α-synuclein against self-aggregation and Ser$^{129}$ phosphorylation. Taken together, these data show that Sept4 may be involved in PD as a dual susceptibility factor, as its insufficiency can diminish dopaminergic neurotransmission and enhance α-synuclein neurotoxicity.**

## INTRODUCTION

Septins are polymerizing GTP binding proteins that serve as scaffolds for diverse molecules beneath the plasma membrane (Field and Kellogg, 1999; Versele and Thorner, 2005; Kinoshita, 2006). In addition to playing roles in mitosis (Kinoshita et al., 1997, Surka et al., 2002; Spiliotis et al., 2005), mammalian septins are abundant in the central nervous system (CNS) (Kinoshita et al., 1998, 2000; Xue et al., 2004; Hall et al., 2005), where they have been implicated in exocytosis (Hsu et al., 1998; Beites et al., 1999, 2005; Xue et al., 2004). However, it is not clear whether and how septins are involved in exocytosis and/or neurotransmission in vivo, partly because mice that lack *Sept3*, *Sept5*, or *Sept6* do not show obvious CNS abnormalities (Fujishima et al., 2007; Peng et al., 2002; Ono et al., 2005).

Meanwhile, septins have been implicated in diverse neurodegenerative disorders in humans. For instance, mutations in the *Sept9* gene were found in hereditary neuralgic amyotrophy (Kuhlenbaumer et al., 2005). Sept4 and two other septins were found in neurofibrillary tangles in Alzheimer's disease (Kinoshita et al., 1998). Sept4 coaggregates with α-synuclein in cytoplasmic inclusion bodies known as Lewy bodies (LBs) in sporadic Parkinson disease (PD) and dementia with Lewy bodies and in glial cytoplasmic inclusions in multiple system atrophy (Ihara et al., 2003). Sept4 and Sept5/CDCrel-1 are substrates for a ubiquitin ligase, parkin; hence, loss of parkin function may result in accumulation of these paralogous septins (Zhang et al., 2000b; Choi et al., 2003; Son et al., 2005). Intriguingly, acute overload of Sept5 can be both inhibitory to exocytosis and neurotoxic (Beites et al., 1999; Dong et al., 2003; Son et al., 2005). However, it is not clear whether the toxicity of septin overload or loss of septin function plays important roles in the pathogenesis of α-synucleinopathies.

This study was designed to address physiological and pathological roles of Sept4 in normal and PD brains. We first examined the status of Sept4 in sporadic PD cases and found that it was often deficient in dopaminergic

(DA) nerve terminals in the striatum. This prompted us to explore the consequences of Sept4 deficiency in *Sept4*$^{-/-}$ mice, and our comprehensive screening pinpointed a specific attenuation of their nigrostriatal DA transmission without affecting the neuronal morphology. We found that Sept4 is required for DA neurons to maintain key components of DA metabolism. Transgenic supplementation of Sept4 was sufficient to rescue the biochemical deficits in *Sept4*$^{-/-}$ striatum. Finally, we tested whether Sept4 deficiency could modify α-synucleinopathy in transgenic mice expressing human α-synuclein$^{A53T}$, a pathogenic mutant responsible for a trait of familial PD (Giasson et al., 2002). Surprisingly, genetic loss of *Sept4* in this PD model exacerbated neuronal loss, gliosis, and locomotor deterioration, which were accompanied by severe amyloid deposits containing Ser$^{129}$-phosphorylated α-synuclein$^{A53T}$. In vitro, Sept4 interfered with self-aggregation and Ser$^{129}$ phosphorylation of α-synuclein. These results suggest that physiological interaction with Sept4 prevents α-synuclein from converting into neurotoxic species and aggregates, and that DA neurons deficient in Sept4 become more susceptible to further dysfunction and degeneration in PD.

## RESULTS

### Physiological Localization of Sept4 in Presynaptic Dopaminergic Terminals in Human Striatum and Its Depletion in Parkinson Disease

In agreement with our previous observations (Ihara et al., 2003), antibodies raised against three distinct epitopes of Sept4 consistently labeled LBs in the substantia nigra pars compacta (SNpc) of all sporadic PD cases examined (n = 5; Figures 1B and 1D, and data not shown). Sept4 and α-synuclein colocalized in the core of LBs (Figures 1C and 1D), indicating their close relationship. In contrast, antibodies for five other septins including Sept5/CDCrel-1 (a substrate for parkin) did not label LBs (Figure 1A and data not shown). These data confirmed the specific involvement of Sept4 in α-synuclein aggregates in PD.

In control human brains without PD, Sept4 was abundant in presynaptic terminals of DA neurons projecting from SNpc to the striatum (putamen). Sept4 was colocalized in the varicosities with the dopamine transporter (DAT in Figures 1E–1G) and α-synuclein (αS in Figures 1H–1J). These data suggest physiological association of Sept4 with these presynaptic molecules in DA nerve terminals.

To examine the status of presynaptic Sept4 in PD, we measured the content of Sept4 in the putamen by immunohistochemistry and immunoblot. In non-PD controls, immunohistochemical signals for Sept4 were more intense in the putamen than in the adjacent cerebral (insular) cortex (Figures 1K and 1S), while in PD, Sept4 was recognizably reduced in the putamen (Figures 1L and 1S). The deficiency of Sept4 was comparable with that of DAT in the adjacent slices (Figures 1Q and 1R). The relative densitometric values for Sept4 in the putamen (Dpu) and insular cortex (Dcx) could segregate PD cases from non-PD controls (Figure 1M, n = 12). In contrast, a general presynaptic marker, synaptophysin, was not reduced in PD putamen (Figures 1N–1P, n = 8). Consistently, immunoblot analysis demonstrated that Sept4 was often reduced in PD specifically in the putamen but not in the cerebral cortex (Figures 1T–1W and Figure S1 in the Supplemental Data). Considering the heterogeneous etiology of sporadic PD and the variability of individual human samples, Sept4 deficiency in the striatum is regarded as one of the common pathological changes in PD.

### Loss of Sept4 Attenuates Dopaminergic Transmission in the Mouse

To address the physiological significance of Sept4 in the CNS, we examined the distribution of Sept4 and the impact of its loss in the mouse. Using in situ hybridization and immunohistochemistry techniques, it was demonstrated that Sept4 was expressed in specific cell populations in the cerebral cortex, striatum, midbrain, cerebellum, and spinal cord (Figures 2A–2E, Figure S9, and data not shown). As with DA neurons, Sept4 was present in the cell bodies in the SNpc and ventral tegmental area (VTA) (Figure 2D), in projection fiber bundles (arrows in Figures 2B and 2E), and in axon terminals surrounding striatal neurons (Figure 2E). As seen in the human brain, Sept4, α-synuclein, and DAT were abundant and colocalized in the axon terminals, especially at the varicosities (Figures 2F–2K).

We generated *Sept4*$^{-/-}$ mice with a genetic background of C57BL/6J, all of which appeared normal except for unexpected male infertility (Ihara et al., 2005). All the Sept4 polypeptides were abolished in *Sept4*$^{-/-}$ brain (Figures 2A–2C). Given the widespread distribution of Sept4 in the CNS, we performed a comprehensive physical and behavioral screening (Supplemental Figures S2–S5). *Sept4*$^{-/-}$ mice were normal except for a paradigm of prepulse inhibition of the acoustic startle response (PPI). This paradigm is an index of reduction in startle amplitude to a loud acoustic stimulus when the stimulus is preceded by a moderate prestimulus (Figure 3A). *Sept4*$^{-/-}$ mice exhibited a lower basal startle response and a significant enhancement in PPI (Figure 3B; p = 0.0011). Since DA antagonists can enhance PPI (Zhang et al., 2000a), we suspected attenuated DA transmission in *Sept4*$^{-/-}$ mice. The mice were challenged with apomorphine at a low dose (0.05 mg/kg) that is known to block DA transmission by selectively stimulating DA presynaptic autoreceptors (Starke et al., 1989). PPI was enhanced in *Sept4*$^{+/+}$ mice but disrupted in *Sept4*$^{-/-}$ mice (the differences between Figures 3B and 3C are indexed in Figure 3D). However, a higher dose of apomorphine (3 mg/kg), which dominantly stimulates postsynaptic DA receptors, disrupted PPI in both genotypes (Supplemental Figure S6). Thus, the attenuated DA transmission in *Sept4*$^{-/-}$ mice was attributed to presynaptic (rather than postsynaptic) defects.

To confirm this, we reassessed spontaneous locomotor activity in an open field (as in Supplemental Figure S5) with methamphetamine, which releases DA from the

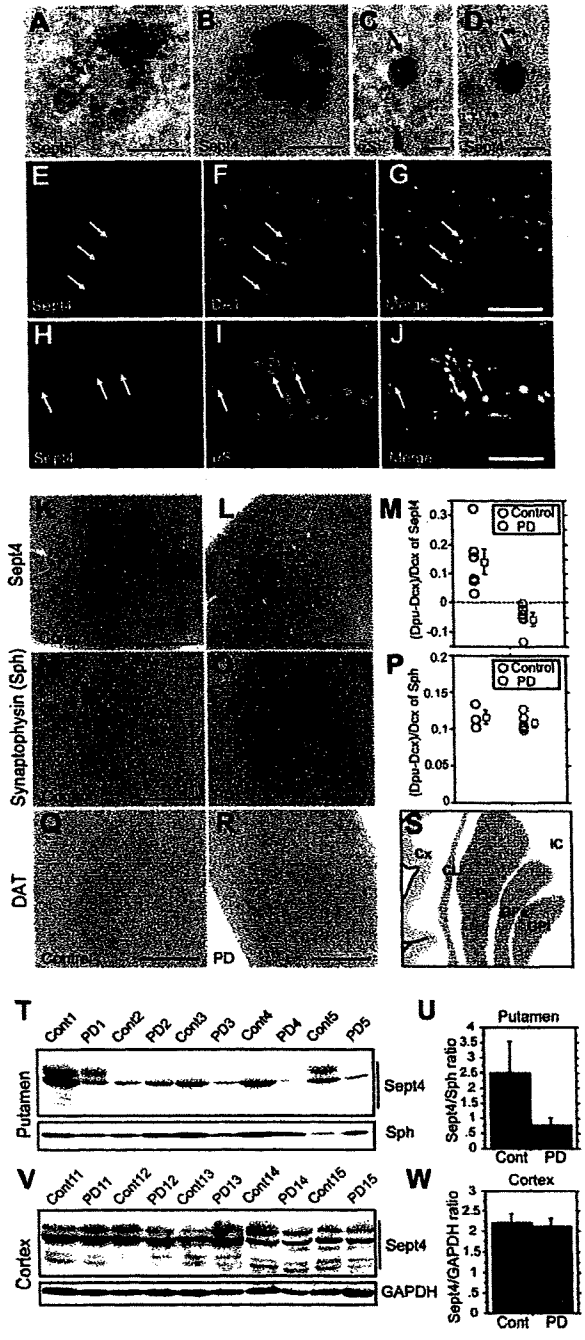


**Figure 1. Involvement of Sept4 in Sporadic Parkinson Disease: Sequestration in Nigral Lewy Bodies and Depletion in the Striatum**

(A and B) Nigral DA neurons bearing LBs in human brains affected with sporadic PD. LBs (arrows), surrounded by neuromelanin granules (dark brown deposits), were not labeled for Sept5 (A), but were consistently labeled for Sept4 (light brown signal in B). Bars, 20 μm.

(C and D) Two adjacent sections showing a DA neuron with an LB (arrows) containing both α-synuclein (αS) (C) and Sept4 (D). Bars, 20 μm.

(E–G) The normal human striatum labeled for Sept4 ([E], red) and the dopamine transporter (DAT) ([F], green) and the merged image [G]. Arrows indicate presynaptic varicosities where intense signals of Sept4 and DAT colocalize. Bar, 20 μm.

(H–J) The normal human striatum labeled for Sept4 ([H], red) and α-synuclein ([I], green) and the merged image (J). Sept4 also colocalized with α-synuclein in presynaptic varicosities (arrows). Bar, 20 μm.

(K and L) Representative images of Sept4 immunohistochemistry in coronally sectioned human brains without (K) and with (L) sporadic PD. Bars, 5 mm.

(M) Semiquantification of the Sept4 signal in the putamen with sporadic PD (n = 6) and without (n = 6). The relative abundance of Sept4 in the striatum is represented by an index, (Dpu-Dcx)/Dcx, where Dpu and Dcx are the densitometric values of Sept4 in the putamen and insular cortex, respectively.

(N–P) Relative striatal content of synaptophysin (Sph), a presynaptic marker protein, was analyzed as in (M). Unlike Sept4, synaptophysin was not depleted from the striatum in PD. Bars, 5 mm.

(Q and R) Immunohistochemistry of DAT in a non-PD (Q) and a PD (R) brain, showing depletion of DAT from the striatum in PD. Bars, 5 mm.

(S) An anatomical diagram of the human basal ganglia (coronal section). Cx, insular cortex; CL, claustrum; Pu, putamen; GPe/GPi, external/internal pallidum; IC, internal capsule.

(T and U) Relative content of Sept4 was quantified by immunoblot in the putamen of sporadic PD (n = 10) and non-PD (n = 10) brains. The densitometric ratio of Sept4/synaptophysin (Sph) was frequently reduced in the striata of the PD patients.

(V and W) Relative content of Sept4 was quantified by immunoblot in the frontal cortex of sporadic PD (n = 5) and non-PD (n = 5) brains. The densitometric ratio of Sept4/GAPDH was not reduced in the cerebral cortices of the PD patients. These data also exclude a possibility that Sept4 is subject to postmortem protein degradation.

presynaptic terminals (Hyman et al., 2006). While the basal activity and methamphetamine-driven hyperactive surge were almost normal in *Sept4*$^{-/-}$ mice, their hyperactivity decayed more rapidly (Figure 3E, $p < 0.05$). These data indicate a presynaptic cause of the attenuated DA transmission in *Sept4*$^{-/-}$ striatum.

In addition, DA content was significantly reduced in *Sept4*$^{-/-}$ striatum by ~25% (Figure 6G; $p = 0.039$), indicating a requirement of Sept4 for DA metabolism.

### Dopaminergic Axon Terminals in *Sept4*$^{-/-}$ Striatum Are Morphologically Normal but Deficient in Key Molecules for Dopamine Metabolism

Based on the behavioral pharmacology data, we examined the status of nigral DA neurons by immunohistochemistry for tyrosine hydroxylase (TH), the rate-limiting enzyme of DA synthesis. In the midbrain, the number and morphology of TH-positive neuronal somata were comparable between *Sept4*$^{+/+}$ and *Sept4*$^{-/-}$ mice (Supplemental Figure S7). However, *Sept4*$^{-/-}$ striatum was labeled less intensely for TH and DAT (Figure 4A). Quantitative morphometric analyses of TH/DAT-positive axons and axon terminals at both the light microscopy level (Figure 4B) and EM level (Figure 4C and Supplemental Figure S8) could not discriminate the two genotypes.

In immunoblot, the densitometric ratios of TH and DAT against synapsin IIa or glyceraldehyde-3-phosphate dehydrogenase (GAPDH) were significantly reduced in *Sept4*$^{-/-}$ striatum (by ~30% and ~55%, respectively),

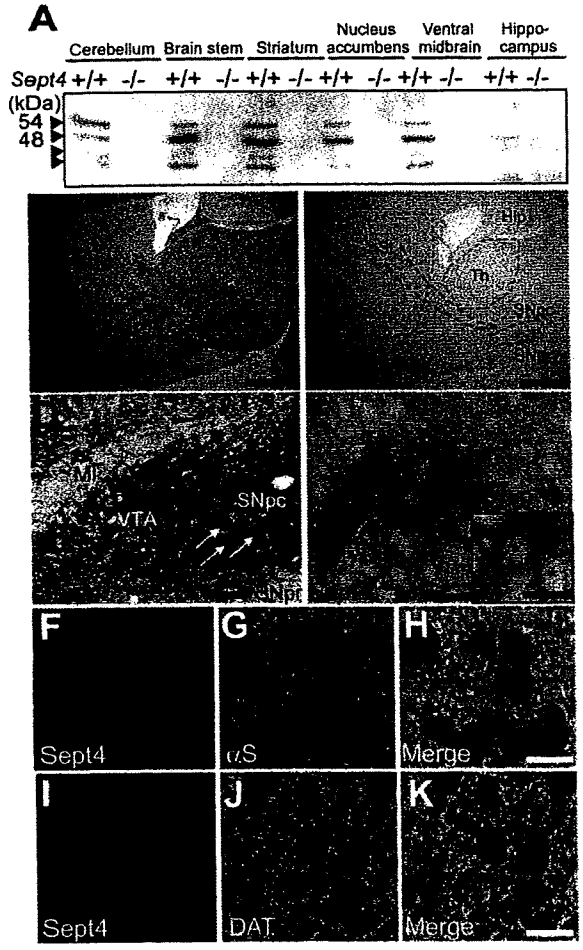


**Figure 2. Expression of Sept4 in the Mouse Brain**

(A) Immunoblot of mouse brain extracts for Sept4. Four *Sept4* products were detected in most parts of the brain to a varying degree and were abolished in *Sept4*$^{-/-}$ mice. Each lane contained 50 μg protein.

(B and C) Sept4 immunohistochemistry (brown signals) in parasagittal sections of *Sept4*$^{+/+}$ and *Sept4*$^{-/-}$ forebrains. The left and top in the figures are the rostral and dorsal aspects, respectively. Projection fiber bundles containing the nigrostriatal pathway are indicated by arrows in (B) and dotted arrows in (C). CCx, cerebral cortex; St, striatum; SNpc, substantia nigra pars compacta; SNpr, substantia nigra pars reticulata; Th, thalamus; Hip, hippocampus. Bars: 1.5 mm.

(D) Sept4 immunohistochemistry using nickel enhancement (blue signals) in a coronal section of *Sept4*$^{+/+}$ ventral midbrain. Sept4 was detected in neuronal cell bodies in the ventral tegmental area (VTA; black arrows) and SNpc (white arrows). Ml, medial lemniscus. Bar: 20 μm.

(E) A parasagittal section of *Sept4*$^{+/+}$ striatum. Note Sept4-containing (brown) puncta in the axon bundles (arrows) and their terminals surrounding the target neurons (asterisks). Bar: 20 μm; inset, 10 μm.

(F–K) Double-label immunofluorescence of presynaptic terminals in *Sept4*$^{+/+}$ striatum. Sept4 signals ([F and I], red) were partially overlapped with those of α-synuclein ([G], green), and DAT ([J], green). Bars: 10 μm (H and K).

but not in the ventral midbrain (Figures 4D–4G; data not shown). However, five postsynaptic parameters we examined were unaffected (Figures 4H and 4I, Figure 6D, and data not shown). These data indicate that loss of Sept4 directly or indirectly reduces the concentration of TH and DAT in DA axons and axon terminals without affecting their morphology. The scarcity of the two essential molecules for DA metabolism may well account for the hypodopaminergic phenotype observed in *Sept4*$^{-/-}$ mice.

### Transgenic Supplementation of Sept4 Can Restore the Deficiency of TH and DAT in *Sept4*$^{-/-}$ Mice

In the next series of experiments, we examined whether Sept4 can rescue the deficiency of TH and DAT in *Sept4*$^{-/-}$ mice. For these purposes, we generated two lines of transgenic mice, *Sept4-Tg1* and *Sept4-Tg2*, each harboring ~10 transcription units of *Sept4*$^{54\ kDa}$ cDNA driven by the prion promoter. The heterozygous Tg mice were lean (~25% body weight reduction), short-lived, and barely fertile. These defects seemed to be due to the nonspecific cytotoxicity of Sept4 overload (Ihara et al., 2003; Dong et al., 2003) and ectopic Sept4 expression in the heart, adrenal gland, and germ cells (see Discussion). Crossbreeding of *Sept4-Tg1* and *Sept4*$^{-/-}$ mice rarely generated live *Sept4KO/Tg1* mice that expressed Sept4$^{54\ kDa}$ and shorter processed forms in the striatum. *Sept4KO/Tg1* striatum contained normal levels of TH and DAT (Figures 5A and 5B). Although *Sept4KO/Tg2* mice were never born, *Sept4-Tg2* mice showed hyper-dopaminergic behaviors (Figures 5C and 5D) and supernormal levels of TH and DAT (data not shown).

Although the primary effects from the loss or excess of Sept4 may be complicated by compensatory and adaptive changes, these data consistently indicate a positive role for Sept4 in DA metabolism.

### Sept4 Is Required as a Component of the Presynaptic Machinery for DA Turnover

To determine the molecular mechanism underlying the hypo-dopaminergic phenotype of *Sept4*$^{-/-}$ mice, we immunoprecipitated striatal homogenates of *Sept4*$^{+/+}$ mice with anti-Sept4 antibodies, then immunoblotted for possible Sept4-interacting molecules. Consistent with our previous report (Ihara et al., 2003) and the colocalization data (Figures 1G and 1J and Figures 2H and 2K), Sept4 was coimmunoprecipitated with DAT and α-synuclein (Figures 6A and 6B). Since Sept5, the closest paralog of Sept4, has been implicated in syntaxin (Stx)-mediated exocytosis (Beites et al., 1999), we tested the interaction between these septins and Stx-1A. Sept5 and Stx-1A were coimmunoprecipitated from the cerebellar cortex, but not from the striatum (data not shown). In contrast, Sept4 and Stx-1A were reciprocally coimmunoprecipitated from the striatum (Figures 6A and 6C). However, a component of the exocyst complex, Sec8, and a postsynaptic protein, mGluR1, were present in the striatum but did not immunoprecipitate with Sept4 (Figure 6A). These data indicate a physiological association of Sept4 with presynaptic molecules involved in DA release and reuptake. Given the individual associations between α-synuclein and DAT (Lee et al., 2001), and Stx-1A and DAT

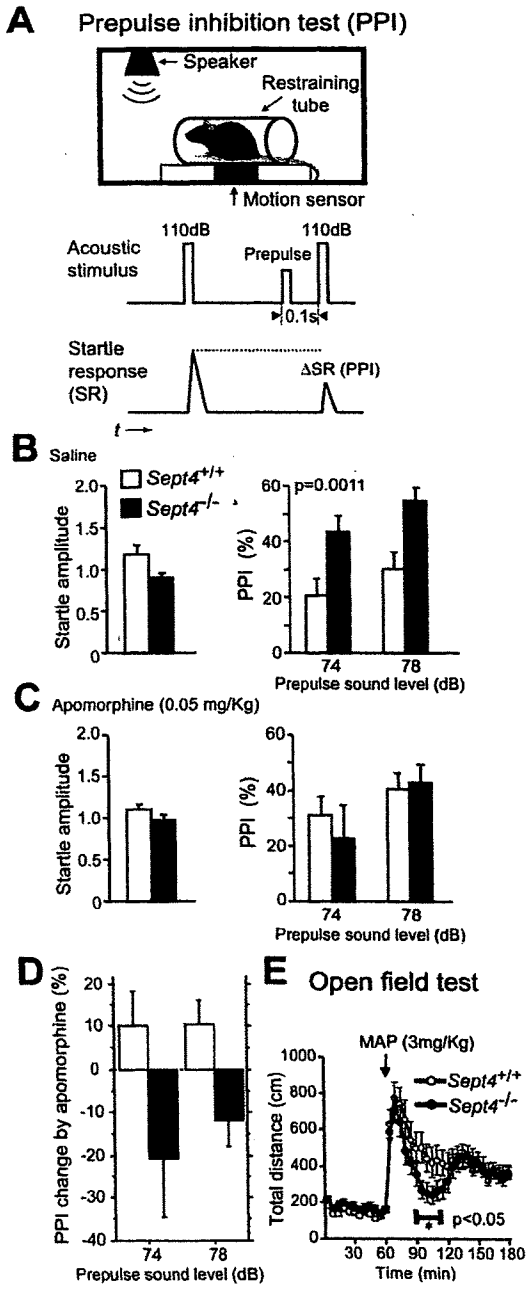


**Figure 3. *Septin4*$^{-/-}$ Mice Exhibit Hypo-Dopaminergic Abnormalities in Prepulse Inhibition and Methamphetamine-Induced Locomotor Response**

(A) (Top) The measurement of PPI of acoustic startle response. (Bottom) PPI is defined here as the percent reduction in the amplitude of the startle response to a loud stimulus (pulse) when it is preceded by a moderate prestimulus (prepulse).

(B) The startle response amplitude to a 110 dB stimulus (left) and PPI (right) after a mock pretreatment with saline. As compared with *Septin4*$^{+/+}$ littermates, *Septin4*$^{-/-}$ mice showed significant enhancement in PPI by a prepulse of 74 or 78 dB (n = 15 per genotype).

(C) The startle amplitude to the 110 dB stimulus (left) and PPI (right) after a pretreatment with a DA agonist, apomorphine (0.05 mg/Kg s.c.). Presynaptic DA blockade by apomorphine enhanced PPI in *Septin4*$^{+/+}$ mice (as seen in *Septin4*$^{-/-}$ mice in B), whereas it paradoxically disrupted PPI in *Septin4*$^{-/-}$ mice.

(D) Comparison of the apomorphine-induced PPI changes by genotype.

(E) Methamphetamine-induced hyperactivity was not sustained in *Septin4*$^{-/-}$ mice. Spontaneous activities of *Septin4*$^{+/+}$ and *Septin4*$^{-/-}$ littermates were automatically measured in an open field setup. After a habituation, methamphetamine (MAP, 3 mg/Kg, i.p.) was injected at $t = 60$ (min, arrow). Although the basal and peak activities of *Septin4*$^{-/-}$ mice were almost normal, locomotion was significantly less than that of *Septin4*$^{+/+}$ littermates for the time block of $t = 85$–$110$ ($F_{1,30} = 4.172$, $p < 0.05$, n = 16 per genotype). The activity of *Septin4*$^{-/-}$ mice recovered to the normal level at $t = 130$ and later.

(Lee et al., 2004), our results point to a larger protein complex in the striatum that contains Sept4, α-synuclein, Stx-1A, and DAT.

Septins often serve as scaffolds that anchor and/or stabilize other molecules. Depletion of cellular septins by RNAi reduces the amount of binding partners in the same complex (Kinoshita et al., 2002). Thus, we examined whether the loss of Sept4 also affects interaction partners other than DAT. In *Septin4*$^{-/-}$ striatum, the contents of Stx-1A, SNAP25, Munc18, and α-synuclein were slightly but consistently reduced, while that of Vesl-1L, a postsynaptic protein, was not affected (Figures 6D–6F). (Note: we predict the deficiencies of Stx-1A and α-synuclein in DA neurons were underestimated by this method; these molecules are also expressed in other cells that do not express Sept4, and are hence unaffected by the loss of Sept4.)

The biochemical evidence, along with the colocalization and behavioral data, strongly suggests that Sept4 is closely associated with the key molecules for DA metabolism. Considering the normal morphology of *Septin4*$^{-/-}$ DA neurons (Figures 4B and 4C and Supplemental Figure S8), Sept4 may be required not as a cytoskeletal protein, but as a component of a presynaptic scaffold that directly or indirectly supports the molecular machinery for dopamine turnover.

### Loss of *Septin4* Exacerbates Neuropathology of *α-Synuclein*$^{A53T}$ Transgenic Mice

Next, we focused on pathological interaction between Sept4 and another molecule in the DA terminals, α-synuclein. We have so far demonstrated their physiological association and pathological coaggregation in α-synucleinopathies (Ihara et al., 2003; and Figures 1B–1D, Figure 2H, and Figures 6A, 6B, 6D, and 6F). To critically test whether the interaction with Sept4 promotes or suppresses aggregation and neurotoxicity of α-synuclein, we utilized *Septin4*$^{-/-}$ mice. We also employed a transgenic mouse model of α-synucleinopathy, in which human α-synuclein$^{A53T}$ (a mutant protein responsible for a trait of familial PD) is expressed by the prion promoter (Giasson et al., 2002). As reported, biallelic *α-synuclein*$^{A53T}$ transgenic mice ($\alpha S^{tg}$ mice) developed locomotor deterioration,

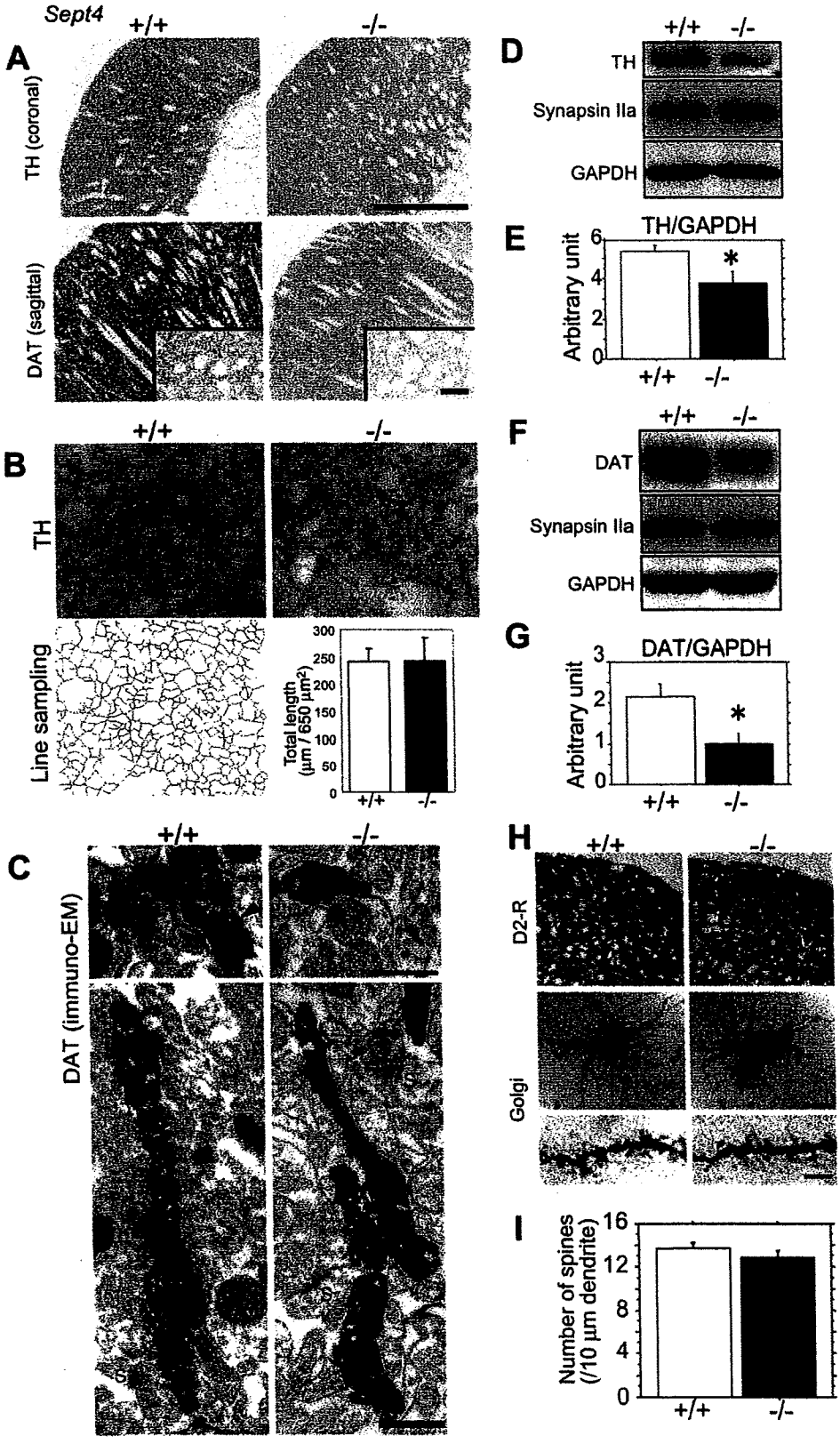
Sept4
+/+
-/-
A
TH (coronal)
DAT (sagittal)
B
TH
Line sampling
Total length (μm / 650 μm²)
C
DAT (immuno-EM)
D
TH
Synapsin IIa
GAPDH
E
TH/GAPDH
Arbitrary unit
F
DAT
Synapsin IIa
GAPDH
G
DAT/GAPDH
Arbitrary unit
H
D2-R
Golgi
I
Number of spines (/10 μm dendrite)

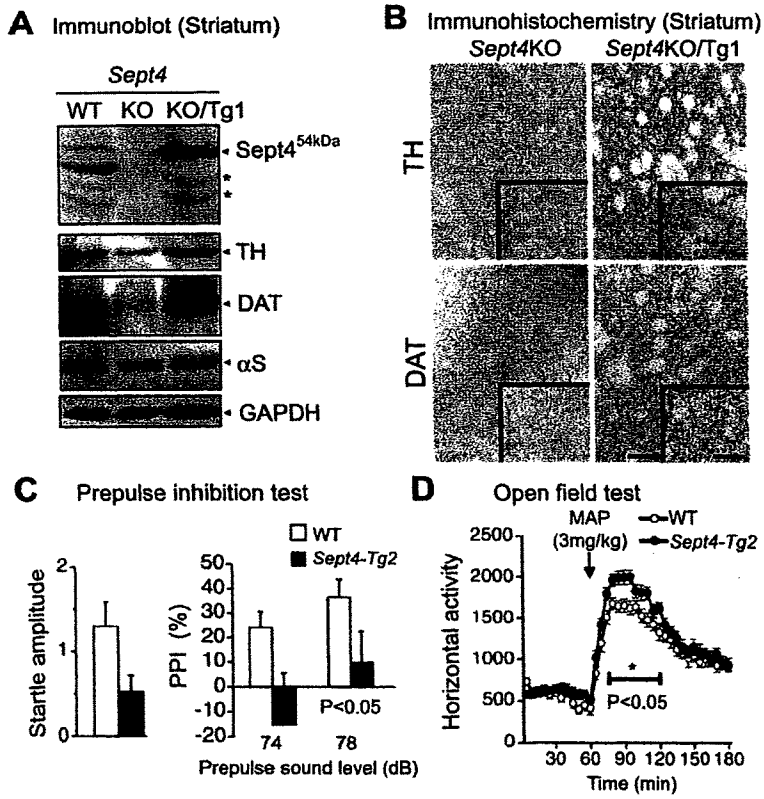


**Figure 5. Transgenic Supplementation of Sept4$^{54\ kDa}$ Can Restore the Scarcity of Presynaptic Molecules in *Sept4*$^{-/-}$ Striatum**

(A) Immunoblot showing the content of Sept4, TH, DAT, α-synuclein (αS), and GAPDH in the striatum of *Sept4*$^{+/+}$ (WT), *Sept4*$^{-/-}$ (KO), and *Sept4*$^{-/-}$/*Sept4*$^{54\ kDa}$ transgenic mice (KO/Tg1). Note that the scarcity of TH and DAT in *Sept4*$^{-/-}$ striatum was reversed by adding back the *Sept4*$^{54\ kDa}$ transgene. The asterisks indicate as of yet uncharacterized processed forms (probably amino-terminal truncations) of Sept4$^{54\ kDa}$. Each lane contained 50 μg protein.

(B) Immunohistochemistry for TH and DAT in the striatum of *Sept4*$^{-/-}$ (KO) and *Sept4*$^{-/-}$/*Sept4*$^{54\ kDa}$ (KO/Tg1) mice. The signal intensities were restored in DA terminals, most obviously in the presynaptic varicosities (compare also with Figures 4A and 4B). Bar: 20 μm; inset, 10 μm.

(C and D) Another line of transgenic mice, *Sept4-Tg2*, exhibited mild hyper-dopaminergic behaviors, i.e., disruption of PPI (C) and hypersensitivity to methamphetamine in the open field test (D). These behaviors, completely opposite to the hypo-dopaminergic phenotype of *Sept4*$^{-/-}$ mice, suggest that Sept4 is a positive determinant of DA neurotransmission.

i.e., hindlimb paralysis followed by quadriparesis, and died within a week after the onset of the symptom. All the symptomatic animals examined exhibited α-synuclein pathology throughout the neuraxis. Of note, Sept4 involvement in α-synuclein aggregates was visualized in this model of α-synucleinopathy (Figure 7A).

We examined consequences of genetic loss of *Sept4* in $\alpha S^{tg}$ mice. Unlike non-Tg mice that lived more than 24 months with or without *Sept4*, $\alpha S^{tg}$ mice lacking *Sept4* ($\alpha S^{tg}/S4^{-/-}$) had significantly shorter half survival time of ~12 months as compared with ~17 months of the original $\alpha S^{tg}$ ($\alpha S^{tg}/S4^{+/+}$) mice (Figure 7B, $p < 0.05$). As reported on the original $\alpha S^{tg}$ mice (Giasson et al., 2002), $\alpha S^{tg}/S4^{-/-}$ mice developed α-synuclein aggregates in the brainstem nuclei and spinal ventral horns (Figure 7C). Intriguingly, however, neuropathology of $\alpha S^{tg}/S4^{-/-}$ mice was distinct both qualitatively and quantitatively from that of $\alpha S^{tg}/S4^{+/+}$ mice in the following four ways.

(1) In the pontine reticular nuclei and spinal ventral horns, $\alpha S^{tg}/S4^{-/-}$ mice developed more amyloid deposits of α-synuclein that contained a pathologically phosphorylated form (pSer$^{129}$αS; Fujiwara et al., 2002) and were

**Figure 4. Loss of Sept4 Attenuates Key Components of Dopamine Metabolism without Affecting the Morphology of DA Neurons**

(A) Comparative immunohistochemistry revealed that the signal intensity for tyrosine hydroxylase (TH) and DAT were reduced in *Sept4*$^{-/-}$ striatum. Bar: 0.5 mm; inset, 20 μm.

(B) Network of axons and axon terminals of DA neurons were faintly labeled for TH but morphologically well-developed in *Sept4*$^{-/-}$ striatum. TH-positive structures were automatically extracted from digital microscopic images (e.g., bottom, left), and the total length of each binary image was quantified and statistically analyzed (bottom, right). There was no difference in the total length of TH-positive structures by genotype. See Experimental Procedures for details. Bar: 20 μm.

(C) Immuno-EM images for DAT in the dorsal striata of *Sept4*$^{+/+}$ and *Sept4*$^{-/-}$ mice. The fine morphology of DA neuron terminals was not different between genotypes. Some DAT-positive presynaptic terminals containing synaptic vesicles are apposed to postsynaptic densities (PSDs, arrowheads) formed in the medium spiny neurons. S, asymmetric nondopaminergic (probably glutamatergic) synapses. The total DAT-positive area measured on immuno-EM images was comparable between *Sept4*$^{+/+}$ and *Sept4*$^{-/-}$ striata (Supplemental Figure S8). Bar: 0.5 μm.

(D and E) Mild reduction of TH content in *Sept4*$^{-/-}$ striatum. Homogenates of *Sept4*$^{+/+}$ and *Sept4*$^{-/-}$ striata were blotted for TH, synapsin IIa, and GAPDH. The TH/GAPDH ratio was significantly reduced in *Sept4*$^{-/-}$ striatum ($p < 0.05$, $n = 5$ per genotype). Each lane contained 50 μg protein.

(F and G) As in (D) and (E), significant reduction of DAT content was confirmed in *Sept4*$^{-/-}$ striatum ($p < 0.01$, $n = 7$ per genotype), which is consistent with the immunohistochemical data in (A). Each lane contained 50 μg protein.

(H and I) In contrast, postsynaptic components were unaffected by the loss of *Sept4*. The intrinsic neurons in *Sept4*$^{-/-}$ striatum were morphologically normal in terms of the number of the medium spiny neurons (data not shown), immunohistochemistry for the dopamine type 2 receptor (D2R, [H]), Golgi impregnation stain (Golgi, [H]), and the density of dendritic spines (I). Bar: top panels, 0.1 mm; middle panels, 20 μm; bottom panels, 3 μm.

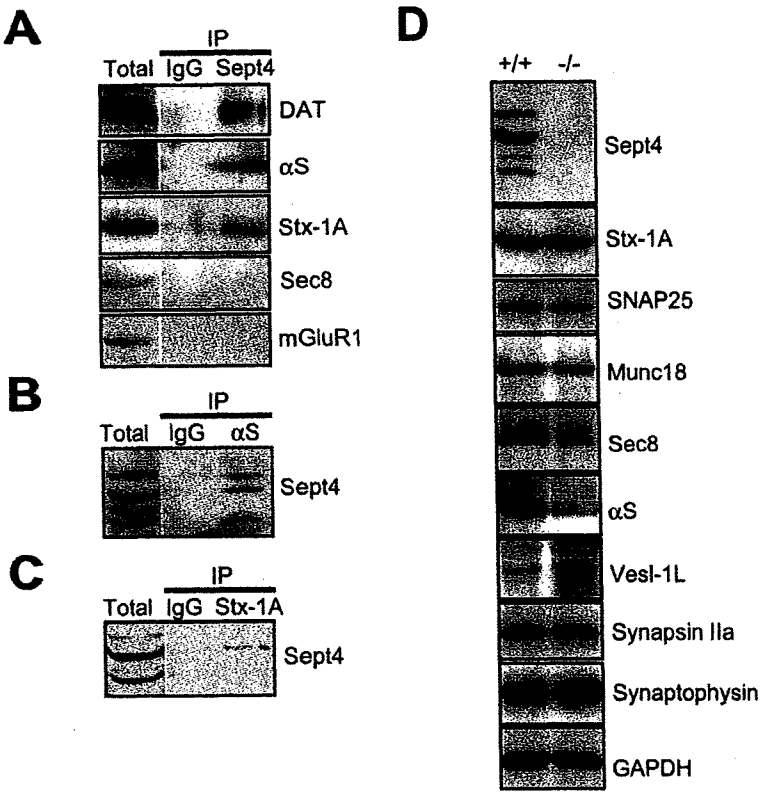


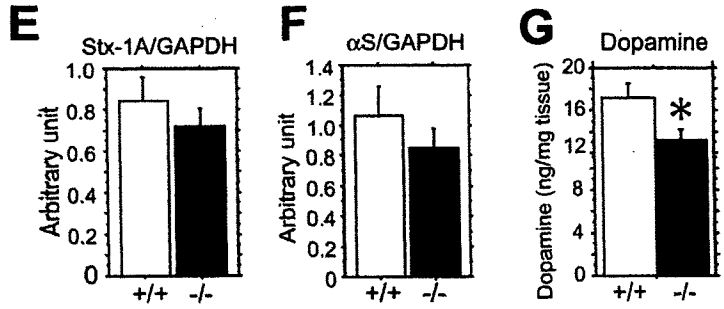


**Figure 6. Selective Scarcity of Proteins for Dopamine Turnover and Dopamine in *Sept4*$^{-/-}$ Striatum**

(A–C) Physical association of Sept4 with DAT, αS, and syntaxin (Stx)-1A in the striatum. (A) *Sept4*$^{+/+}$ striatal homogenate was immunoprecipitated with preimmune rabbit IgG (negative control) or the rabbit polyclonal antibody H5C2 for Sept4, and probed for proteins as indicated. (B and C) The same homogenate was immunoprecipitated with mouse IgG (negative control) and mouse monoclonal antibodies for αS (B) or Stx-1A (C), and probed for Sept4.

(D) Immunoblot of *Sept4*$^{+/+}$ (+/+) and *Sept4*$^{-/-}$ (−/−) striatal homogenates for pre- and postsynaptic proteins.

(E and F) The densitometric ratios of Stx-1A/GAPDH (E) and αS/GAPDH (F) were slightly reduced in *Sept4*$^{-/-}$ striata (n = 5 per genotype). Because Stx-1A and αS are ubiquitous in the brain, their scarcity in *Sept4*$^{-/-}$ DA terminals seems to be obscured.

(G) DA content measured by HPLC was significantly reduced in *Sept4*$^{-/-}$ striatum by 25% (p = 0.039, n = 5 per genotype). There was a similar trend in the nucleus accumbens, another target of nigral DA neurons (data not shown).

resistant to digestion by proteinase K (Figure 7C, top panels, and Supplemental Figure S11). (2) In the spinal ventral horns, *αS*$^{tg}$/*S4*$^{-/-}$ mice exhibited a significant loss of large motor neurons (>20 μm in diameter); however, smaller motor neurons and interneurons were not affected (~5–20 μm) (Figure 7C, bottom panels, and Figure 7D). (3) In the spinal ventral horns, *αS*$^{tg}$/*S4*$^{-/-}$ mice exhibited more severe astrocytic gliosis, indicative of ongoing inflammatory and degenerative processes (Supplemental Figure S10). (4) In the SNpc of *αS*$^{tg}$/*S4*$^{-/-}$ mice, pSer$^{129}$αS-positive aggregates were formed in DA neurons and swollen neurites (Figure 7F), and were not found in *αS*$^{tg}$/*S4*$^{+/+}$ mice. These data indicate that *Sept4* can be regarded as a suppressor of neurodegeneration by *α-synuclein*$^{A53T}$ overload.

### Sept4 Can Suppress Pathological Modifications of α-Synuclein In Vivo

To analyze the molecular basis of the enhancement of α-synuclein pathology by the loss of *Sept4*, we examined the biochemical status of α-synuclein in graded extraction (i.e., in Triton-soluble, sodium dodecyl sulfate- [SDS-] soluble, and SDS-insoluble fractions) of the spinal cord. In each fraction of young asymptomatic mice, α-synuclein was detected mainly as the native form of ~17 kDa (αS in Figure 7E, left top panel). Intriguingly, the SDS-insoluble fraction of aged, symptomatic mice additionally contained putative crosslinked dimers [$(αS)_2$] and other modified forms, high-molecular-weight smears (HMWαS), and aggregates that stuck at the top of the resolving gel (arrow in Figure 7E, right top panel). These aberrant α-synuclein

species were more prominent in symptomatic $\alpha S^{tg}/S4^{-/-}$ mice than in older symptomatic $\alpha S^{tg}/S4^{+/+}$ mice (compare the second and third lanes from the right in Figure 7E, right top panel). The modified α-synuclein species were reminiscent of those found in human α-synucleinopathies; i.e., the ~24 kDa band may correspond to O-glycosylation (Shimura et al., 2001) or another modification (Tofaris et al., 2003), and the ~40 kDa double bands may represent crosslinked homodimers and/or other modified species (Kahle et al., 2001). None of these modified species were labeled for ubiquitin (data not shown).

Among other biochemical abnormalities, accumulation of $pSer^{129}\alpha S$ in the SDS-insoluble fraction was the most significant characteristic of symptomatic $\alpha S^{tg}/S4^{-/-}$ mice (Figure 7E, right second panel). The amount of insoluble $pSer^{129}\alpha S$ was positively correlated with the severity of neuropathology in the spinal cord. Thus, SDS-insoluble $pSer^{129}\alpha S$ seems to correspond to the protease-resistant amyloid deposits (Figure 7C and Supplemental Figure S11). $\alpha S^{tg}$ mice hemizygous for *Sept4* ($\alpha S^{tg}/S4^{+/-}$) contained an intermediate amount of $pSer^{129}\alpha S$ in each fraction (Supplemental Figure S12), indicating that the dosage of Sept4 is a determinant of α-synuclein modification. Importantly, symptomatic $\alpha S^{tg}/S4^{-/-}$ mice contained SDS-insoluble $pSer^{129}\alpha S$ not only in the spinal cord, but also in the forebrain (data not shown) and the nigral DA neurons in the midbrain (Figures 7F–7H).

Taken together, aggregation and $Ser^{129}$ phosphorylation of α-synuclein seem to be central events underlying the neurodegeneration of $\alpha S^{tg}$ mice, and these pathological modifications were obviously enhanced by the loss of Sept4.

### Direct Interaction with Sept4 Prevents Self-Aggregation and $Ser^{129}$ Phosphorylation of α-Synuclein In Vitro

How does Sept4 suppress neurotoxicity caused by chronic overload of α-synuclein? It has been hypothesized that self-aggregation of α-synuclein that occurs in various pathological processes generates neurotoxic species (Dawson and Dawson, 2003), and that $Ser^{129}$ phosphorylation can facilitate the process (Fujiwara et al., 2002). Thus, we tested in vitro whether these modifications could be suppressed by Sept4. First, we confirmed that α-synuclein and Sept4 directly associate in vitro (Figure 8A). Second, we found that Sept4 suppressed self-aggregation of $\alpha\text{-synuclein}^{A53T}$ into SDS-resistant HMW species (Figure 8B). Third, Sept4 partially interfered with $Ser^{129}$ phosphorylation of $\alpha\text{-synuclein}^{A53T}$ by a ubiquitous Ser/Thr-kinase, casein kinase II (CKII; Fujiwara et al., 2002) (Figure 8C). However, Sept4 did not essentially inhibit the kinase activity of CKII when casein was used as the substrate (Supplemental Figure S13). When the data were taken together, we concluded that direct interaction with Sept4 can prevent α-synuclein from self-aggregation (as has been proposed for another LB component, αB-crystallin) (Rekas et al., 2004), and may shield α-synuclein from $Ser^{129}$ phosphorylation by CKII and other kinases. Such protective effects on α-synuclein modifications, perhaps by steric hindrance and/or conformational changes, may be more effective in the physiological situation where Sept4, DAT, and Stx-1A are in close proximity to α-synuclein (Figure 6A).

## DISCUSSION

### *Sept4*$^{-/-}$ Mice Revealed a Physiological Septin Function in the Brain

Septins have been implicated in exocytosis based on their presynaptic localization (Kinoshita et al., 2000; Xue et al., 2004), physical and functional interaction with syntaxins (Beites et al., 1999, 2005), and aberrant exocytosis in blood platelets lacking Sept5 (Dent et al., 2002). However, previous attempts to address septin functions in the brain with *Sept3*$^{-/-}$, *Sept5*$^{-/-}$, or *Sept6*$^{-/-}$ mice were unsuccessful, probably due to compensation by their functionally redundant paralogs (Fujishima et al., 2007; Peng et al., 2002; Ono et al., 2005). We employed a comprehensive behavioral test as a means of unbiased screening for neurological defects in *Sept4*$^{-/-}$ mice. This approach has successfully pinpointed a specific neurological phenotype by the loss of septin function, i.e., the attenuation of nigrostriatal DA transmission. While DA neurons were functionally affected by the loss of Sept4, non-DA neurons were unchanged. This intriguing form of selectivity may be due to the absence of redundant septin species, and/or a specific requirement of Sept4 subunit, in DA neurons.

### Sept4 Is Required as a Component of Presynaptic Scaffolds in DA Neurons

Extending our previous finding of Sept4 involvement in LBs (Ihara et al., 2003), the present study has revealed Sept4 insufficiency in presynaptic DA terminals in the human striatum affected with sporadic PD. This is partly due to sequestration of Sept4 into α-synuclein aggregates, and partly as a result of neuronal loss. To investigate the pathophysiological impact of Sept4 depletion in PD, we created and investigated several mouse models: the genetic loss of *Sept4* attenuated, an excess of Sept4 enhanced, and a transgenic Sept4 supplementation of *Sept4* null mice normalized nigrostriatal DA transmission. These results suggest a positive role for Sept4 in dopamine turnover.

The hypo-dopaminergic behavioral deficits observed in *Sept4*$^{-/-}$ mice were attributed not to morphological anomalies of DA neurons but to an insufficiency of specific components in DA terminals. The levels of DAT, TH, α-synuclein, Stx-1A, and another tSNARE component depended more or less on the amount of Sept4. Sept4 directly or indirectly interacts with most of these molecules in the striatum. Considering the physical association of these molecules, Sept4 can be regarded as a pivotal component of the presynaptic scaffold for the machinery of dopamine release and reuptake. The detailed organization of such machinery would be an intriguing subject for future studies.

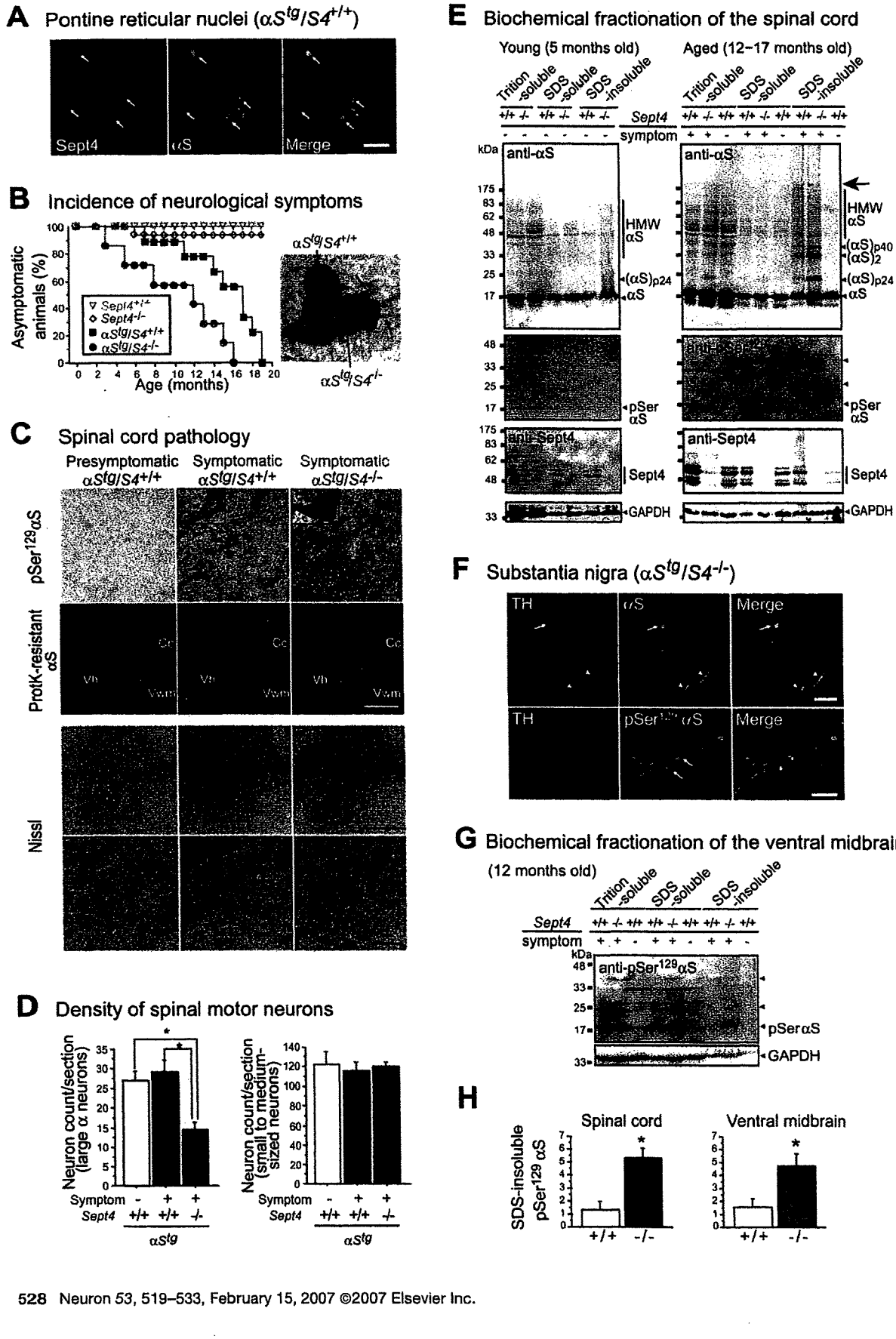
A Pontine reticular nuclei (αS^tg/S4^+/+)
Sept4
αS
Merge
B Incidence of neurological symptoms
Asymptomatic animals (%)
Age (months)
Sept4+/+
Sept4-/-
αStg/S4+/+
αStg/S4-/-
αStg/S4+/+
αStg/S4-/-
C Spinal cord pathology
Presymptomatic αStg/S4+/+
Symptomatic αStg/S4+/+
Symptomatic αStg/S4-/-
pSer129αS
ProtK-resistant αS
Nissl
Cc
Vh
Vsm
D Density of spinal motor neurons
Neuron count/section (large α neurons)
Neuron count/section (small to medium-sized neurons)
Symptom
Sept4
αStg
E Biochemical fractionation of the spinal cord
Young (5 months old)
Aged (12–17 months old)
Trition -soluble
SDS -soluble
SDS -insoluble
Sept4
symptom
kDa
anti-αS
HMW αS
(αS)p24
αS
(αS)p40
(αS)2
anti-pSer αS
pSer αS
anti-Sept4
Sept4
GAPDH
F Substantia nigra (αS^tg/S4^-/-)
TH
αS
Merge
pSer129 αS
G Biochemical fractionation of the ventral midbrain
(12 months old)
anti-pSer129αS
pSerαS
GAPDH
H
SDS-insoluble pSer129 αS
Spinal cord
Ventral midbrain
+/+
-/-

### Physiological and Pathological Interaction between Sept4 and α-Synuclein

α-Synuclein, a presynaptic protein of unknown physiological function, is a soluble, natively unfolded polypeptide. Our study demonstrated physical interaction between α-synuclein and Sept4 in presynaptic terminals of nigral DA neurons. A recent report proposed that α-synuclein might act as a molecular chaperone for some tSNARE components, as excessive α-synuclein prevented the presynaptic degeneration in *CSPα*$^{-/-}$ mice (Chandra et al., 2005). The close association of Sept4 with both α-synuclein and tSNAREs suggests that Sept4 is involved in the proposed scheme. The similar hypo-dopaminergic phenotypes observed in *Sept4*$^{-/-}$ and *α-synuclein*$^{-/-}$ mice (Abeliovich et al., 2000) also support a functional convergence of these molecules.

Under pathological conditions where α-synuclein is overloaded and/or displaced in DA neurons, the polypeptide is subject to various modifications. Above all, Ser$^{129}$ phosphorylation commonly found in LBs/Lewy neurites is considered the hallmark of α-synucleinopathies because pSer$^{129}$αS is absent in normal presynaptic terminals and prone to form aggregates in vitro (Fujiwara et al., 2002). Our data suggest that Sept4 and α-synuclein are components of presynaptic complexes at the DA terminals, and that lack of the physiological association with Sept4 facilitates self-aggregation and Ser$^{129}$ phosphorylation of α-synuclein.

### How Is Sept4 Involved in α-Synucleinopathy?

This study demonstrated that $\alpha S^{tg}$ and $\alpha S^{tg}/S4^{-/-}$ mice provide important insights into the biochemical processes underlying α-synucleinopathies. We have demonstrated that endogenous Sept4 is involved in α-synuclein aggregates formed in $\alpha S^{tg}$ mice (Figure 7A) as well as humans with sporadic PD (Ihara et al., 2003; Figure 1B–1D). The increased α-synuclein aggregation in $\alpha S^{tg}/S4^{-/-}$ mice indicates that Sept4 incorporation is a secondary event that can suppress further α-synuclein aggregation. Based on these and other findings, we propose a model for α-synucleinopathies (Figure 8D), whereby incipient α-synuclein aggregates formed in DA neurons adsorb Sept4. This may retard LB formation, but it eventually depletes Sept4 from the presynaptic terminals (Figure 1K–1U). As seen in $\alpha S^{tg}/S4^{-/-}$ mice, Sept4 insufficiency attenuates DA transmission and subjects α-synuclein to toxic conversions. Thus, pathological α-synuclein/Sept4 interaction in LBs and dissociation of their physiological interaction at presynaptic terminals may constitute a vicious cycle that further disrupts homeostasis of DA neurons in PD.

**Figure 7. Loss of Sept4 Exacerbates Neuropathology and Aberrant α-Synuclein Modifications in *α-synuclein*$^{A53T}$ Transgenic Mice**

(A) Representative α-synuclein aggregates formed in a symptomatic $\alpha S^{tg}/S4^{+/+}$ mouse, 12 months old (m.o.). Coaggregation of Sept4 (red) with αS (green), as seen in human LBs, is recapitulated in this model of α-synucleinopathy. Bar, 20 μm.

(B) (Left) A chart showing the age of onset of hindlimb paresis in $\alpha S^{tg}$ mice with or without *Sept4*. The *Sept4*$^{+/+}$ and *Sept4*$^{-/-}$ non-Tg mice (green and pink plots, respectively) never showed the symptom. Intriguingly, however, $\alpha S^{tg}/S4^{-/-}$ mice (red) developed hindlimb paresis and died 3–4 months earlier than the original $\alpha S^{tg}/S4^{+/+}$ mice (blue; Giasson et al., 2002). (Right) A 12 m.o. $\alpha S^{tg}/S4^{+/+}$ presymptomatic mouse rearing on its $\alpha S^{tg}/S4^{-/-}$ littermate, which had developed hindlimb paresis (arrows).

(C) (First and second panels from top) Representative images of the spinal ventral horn comparatively immunostained for pSer$^{129}$αS (brown) or labeled for total αS after proteinase K digestion (green fluorescence). Each inset shows a pSer$^{129}$αS-positive large motor neuron in the ventral horn (arrowheads); compare the levels of pSer$^{129}$αS and misfolded αS deposits in a 12 m.o. presymptomatic $\alpha S^{tg}/S4^{+/+}$ mouse (left panels), a 16 m.o. symptomatic $\alpha S^{tg}/S4^{+/+}$ mouse (middle panels), and a 12 m.o. symptomatic $\alpha S^{tg}/S4^{-/-}$ mouse (right panels). Bar: upper panels, 40 μm; lower panels, 200 μm. Vh, ventral horn; Vwm, ventral white matter; Cc, central canal. (Third and fourth panels from top) Representative Nissl-stained sections of the spinal cord from the same animals. Note a recognizable reduction of large motor neurons in the symptomatic $\alpha S^{tg}/S4^{-/-}$ mouse (right panels). Bar: upper panels, 200 μm; lower panels, 60 μm.

(D) The counts of large neurons (left) and small to medium-sized neurons (right) in the spinal cord sections from presymptomatic $\alpha S^{tg}/S4^{+/+}$ mice (white bars, 5–8 m.o.), symptomatic $\alpha S^{tg}/S4^{+/+}$ mice (blue bars, 12–18 m.o.), and symptomatic $\alpha S^{tg}/S4^{-/-}$ mice (red bars, 10–14 m.o.). Note that large neurons, classified as α motor neurons, were selectively and significantly lost in $\alpha S^{tg}/S4^{-/-}$ mice (*$p < 0.05$, $n = 4$ per genotype).

(E) (Left, top) The spinal cord homogenates of young presymptomatic $\alpha S^{tg}/S4^{+/+}$ and $\alpha S^{tg}/S4^{-/-}$ littermates were fractionated into Triton (X-100)-soluble, SDS-soluble, and SDS-insoluble components. Each fraction was immunoblotted for total αS, pSer$^{129}$αS, Sept4, and GAPDH. The SDS-insoluble fraction of $\alpha S^{tg}/S4^{-/-}$ mice consistently contained low- to high-molecular-weight (HMW) smear of αS (rightmost lane). (Left, second panel) At this age, αS was barely Ser$^{129}$ phosphorylated in any fraction/genotype measured. Thus, Ser$^{129}$ phosphorylation is preceded by some other modifications that cause the mobility shift of αS. (Right, top) Likewise, $\alpha S^{tg}/S4^{+/+}$ (17 m.o.) and $\alpha S^{tg}/S4^{-/-}$ (12 m.o.) mice with or without symptoms were analyzed. In addition to prominent HMW smears of αS, the SDS-insoluble fractions of the symptomatic animals of each genotype contained larger aggregates at the top of the resolving gel (arrow) and above in the stacking gel. However, only symptomatic $\alpha S^{tg}/S4^{-/-}$ mice contained heavy bands of modified αS (p40, crosslinked dimer, p24; arrowheads) in the SDS-insoluble fraction. (Right, second panel) The aged symptomatic animals commonly contained pSer$^{129}$αS in the Triton-soluble and SDS-soluble fractions. In addition, symptomatic $\alpha S^{tg}/S4^{-/-}$ mice contained significant pSer$^{129}$αS (monomer and higher molecular weight species; arrowheads) in the SDS-insoluble fraction. (Right, third panel) Sept4 in the SDS-insoluble fraction was increased and smeared in symptomatic $\alpha S^{tg}/S4^{+/+}$ mice, reflecting some biochemical modifications and coaggregation with αS.

(F) Double-label immunofluorescence for TH (red) and αS or pSer$^{129}$αS (green) in $\alpha S^{tg}/S4^{-/-}$ SNpc. αS/pSer$^{129}$αS-positive aggregates in DA neurons, which were reminiscent of LBs (arrows) and Lewy neurites (arrowheads), were often found in $\alpha S^{tg}/S4^{-/-}$ ventral midbrain, but never in $\alpha S^{tg}/S4^{+/+}$ mice (data not shown). Bars: upper panels, 40 μm; lower panels, 20 μm.

(G) The ventral midbrains (containing DA neurons in SNpc and VTA) were analyzed as in (E). Intriguingly, each fraction of symptomatic $\alpha S^{tg}/S4^{-/-}$ mice contained more pSer$^{129}$αS (monomer and higher molecular weight species; arrowheads) than that of $\alpha S^{tg}/S4^{+/+}$ mice.

(H) Experiments of (E) and (G) were triplicated and quantified. The densitometric ratio of pSer$^{129}$αS/GAPDH in the SDS-insoluble fraction was significantly higher in the spinal cord and ventral midbrain of symptomatic $\alpha S^{tg}/S4^{-/-}$ mice (−/−) as compared with symptomatic $\alpha S^{tg}/S4^{+/+}$ mice (+/+; *$p < 0.01$, $n = 3$).

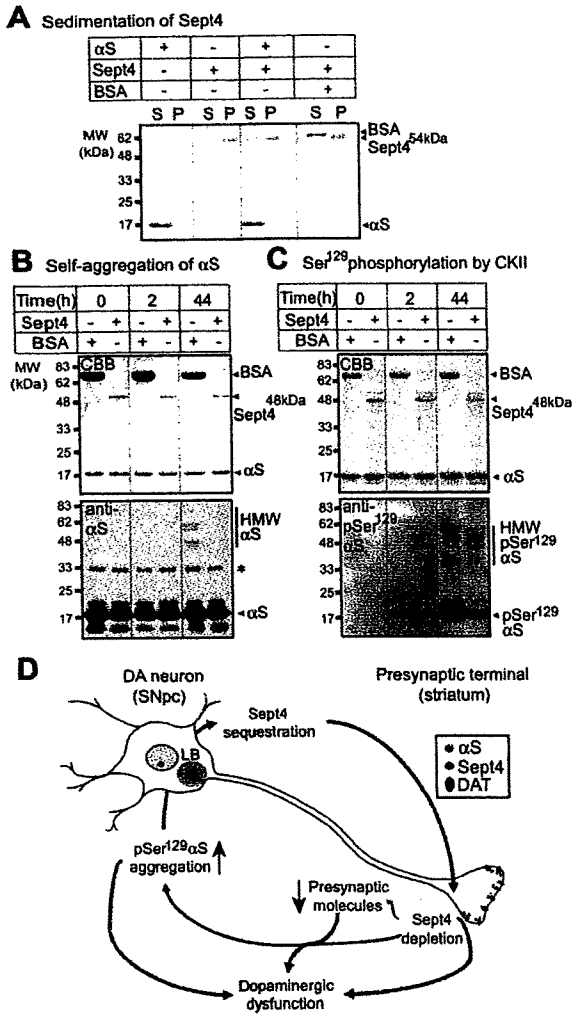


**Figure 8. Sept4 Directly Interacts with α-Synuclein and Suppresses Its Self-Aggregation and Ser$^{129}$ Phosphorylation In Vitro**

(A) Sept4 directly interacts with αS. Mixtures of αS (wild-type), Sept4$^{54\ kDa}$, or BSA in PBS were ultracentrifuged at 440,000 × g for 30 min. The supernatant (S) and the pellet (P) of each mixture were analyzed by SDS-PAGE and stained with Coomassie Brilliant Blue (CBB). (From left to right lanes) αS alone was soluble (S). Most of Sept4 was sedimented (P), perhaps due to homo-oligomerization. αS interacted with Sept4 and interfered with the sedimentation. BSA, another soluble protein used as a control, did not show such effects. These data indicate direct association between Sept4 and αS.

(B) Sept4 can suppress self-aggregation of αS in vitro. (Top and middle panels) Recombinant human α-synuclein$^{A53T}$ (αS) was incubated in a physiological buffer with recombinant Sept4$^{48\ kDa}$ or BSA. Each reaction was resolved by SDS-PAGE and CBB stained. (Bottom panel) The same reactions were immunobloted for total αS. After 44 hr incubation without Sept4, a fraction of αS was self-aggregated or oligomerized as HMW bands. In contrast, HMW bands of αS were not formed in the presence of Sept4. A 34 kDa band (*) represents αS dimers formed in *E.coli* (Masuda et al., 2006).

(C) Sept4 can mildly interfere with casein kinase II (CKII)-mediated phosphorylation and other modifications of α-synuclein in vitro. (Top and middle panels) αS$^{A53T}$, CKII, and ATP were incubated in a buffer with recombinant Sept4$^{48\ kDa}$ or BSA, and analyzed as in (A). (Bottom panel) The same reactions were immunobloted for pSer$^{129}$αS. Sept4 mildly interfered with Ser$^{129}$phosphorylation of αS$^{A53T}$ and the formation of HMW species containing pSer$^{129}$αS. These data also suggested that pSer$^{129}$αS is more prone to self-aggregation than αS (compare the rightmost lanes of B and C). Parallel reactions using wild-type αS (instead of αS$^{A53T}$) gave similar results (data not shown). Data in (A)–(C) are representative of at least three experiments.

(D) A working model of PD pathophysiology including Sept4 as a novel player: α-synuclein aggregates (LB) formed by various pathological causes commonly involve Sept4. The involvement may retard the process while it sequesters and depletes Sept4 from DA nerve terminals in the striatum. The insufficiency of Sept4 in the presynaptic scaffold reduces the critical components for DA transmission, which contributes to DA dysfunction. In addition, an excess of α-synuclein in the absence of Sept4 facilitates its oligomerization, phosphorylation, and other modifications, which generate neurotoxic species.

Intriguingly, DA neurons in αS$^{tg}$ mice developed α-synuclein aggregates only in the absence of Sept4 (Figures 7F–7H). Thus, loss of Sept4 is a critical event for the development of α-synuclein pathology in DA neurons, although it appears additional insults and/or aging are necessary for them to die. When compared with mice, human DA neurons are more sensitive to various insults, including α-synuclein overload (LaVoie et al., 2005; Moore et al., 2005). Thus, Sept4 depletion found in humans (Figures 1K–1U) should impact DA neurons more seriously.

### Loss of Sept4 Function versus Gain of Toxic Effects

*Sept4-Tg1* and *Sept4-Tg2* transgenic mice generated in this study have demonstrated that mild chronic overload of Sept4 is cytotoxic to various cell lineages. This is consistent with previous findings that acute Sept5 overexpression can damage DA neurons in the rat (Dong et al., 2003). Thus, both insufficiency and excess of Sept4 could perturb the homeostasis of DA neurons, ultimately leading to disorganization of their presynaptic terminals—another intriguing similarity to α-synuclein (Abeliovich et al., 2000; Chandra et al., 2005; Moore et al., 2005). As for sporadic PD cases, however, we have not obtained any samples that contained excessive Sept4 in the striatum. Thus, Sept4 overload may not be relevant in the etiology of sporadic PD.

In summary, our present as well as previous studies have established physiological and pathological roles of Sept4 in the nigral DA neurons. Future studies should characterize the presynaptic complex containing Sept4 and other key molecules. From a pathological aspect, unraveling the precise molecular mechanism by which Sept4 suppresses the α-synuclein toxicity may help develop neuroprotective strategies for PD.

## EXPERIMENTAL PROCEDURES

### Analyses of Clinical Samples

Postmortem human brain tissues were dissected within 6 hours postmortem under signed informed consent from the patients' relatives, and in accordance with the guidelines of ethics committees of Kyoto University and Juntendo University. Tissues for immunohistochemistry were fixed at Kyoto University Hospital. Donor subjects included 16 PD